

Fractal and multifractional-based predictive optimization model for stroke subtypes' classification

Yeliz Karaca^{a,1,*}, Majaz Moonis^a, Dumitru Baleanu^{b,c}

^a University of Massachusetts Medical School (UMASS), Worcester, MA 01655, USA

^b Çankaya University, Department of Mathematics, Ankara 1406530, Turkey

^c Institute of Space Sciences, Magurele, Bucharest, Romania

ARTICLE INFO

Article history:

Received 3 October 2019

Revised 20 March 2020

Accepted 13 April 2020

Available online 14 May 2020

Keywords:

Box-counting method

Feedforward neural networks

Fractal dimension

Multifractals

Stroke subtypes

Wavelet transform modulus maxima

ABSTRACT

Numerous natural phenomena display repeating self-similar patterns. Fractal is used when a pattern seems to repeat itself. Fractal and multifractal methods have extensive applications in neurosciences in which the prevalence of fractal properties like self-similarity in the brain, equipped with a complex structure, in medical data analysis at various levels of observation is admitted. The methods come to the fore since subtle details are not always detected by physicians, but these are critical particularly in neurological diseases like stroke which may be life-threatening. The aim of this paper is to identify the self-similar, significant and efficient attributes to achieve high classification accuracy rates for stroke subtypes. Accordingly, two approaches were implemented. The first approach is concerned with application of the fractal and multifractal methods on the stroke dataset in order to identify the regular, self-similar, efficient and significant attributes from the dataset, with these steps: a) application of Box-counting dimension generated BC_stroke dataset b) application of Wavelet transform modulus maxima generated WTMM_stroke dataset. The second approach involves the application of Feed Forward Back Propagation (FFBP) for stroke subtype classification with these steps: (i) FFBP algorithm was applied on the stroke dataset, BC_stroke dataset and WTMM_stroke dataset. (ii) Comparative analyses were performed based on accuracy, sensitivity and specificity for the three datasets. The main contribution is that the study has obtained the identification of self-similar, regular and significant attributes from the stroke subtypes datasets by following multifarious and integrated methodology. The study methodology is based on the singularity spectrum which provides a value concerning how fractal a set of points are in the datasets (BC_stroke dataset and WTMM_stroke dataset). The experimental results reveal the applicability, reliability and accuracy of our proposed integrated method. No earlier work exists in the literature with the relevant stroke datasets and the methods employed. Therefore, the study aims at pointing a new direction in the relevant fields concerning the complex dynamic systems and structures which display multifractional nature.

© 2020 Elsevier Ltd. All rights reserved.

1. Introduction

Fractal geometry is regarded as a universal language employed extensively for analysing and quantifying geometric complexity of natural objects among which the human brain is also included [1]. As has been acknowledged, human brain is a complex system concerning its topological and functional structure, and for this reason, human brain is under detailed investigation in different fields [1]. The fractal geometry notions are utilized in many areas of re-

search [2] and they have been proven to be beneficial quantitative methods for image analysis in the field of medical sciences. Computational analyses based on fractal have also been applied to diverse subfields of neurosciences [3–5]. To illustrate, in many medical data analysis applications, the methods are used for texture analysis, pattern recognition and segmentation. Thus, the quantification and characterization of the brain through the fractal dimension analysis has been a field of growing interest over the recent years [6].

Fractal methods are appealing owing to their ability to describe fragmented or irregular shape of natural features and also other types of complex objects which traditional Euclidean geometry fails to analyse. The fractal analysis is a contemporary method in mathematics used for measuring complexity in nature [7], and this analysis is reliant on fractal geometry [2]. Fractal dimension is the

* Corresponding author.

E-mail addresses: yeliz.karaca@ieee.org (Y. Karaca), majaz.moonis@umassmemorial.org (M. Moonis), dumitru@cankaya.edu.tr (D. Baleanu).

¹ ORCID(S): 0000-0001-8725-6719

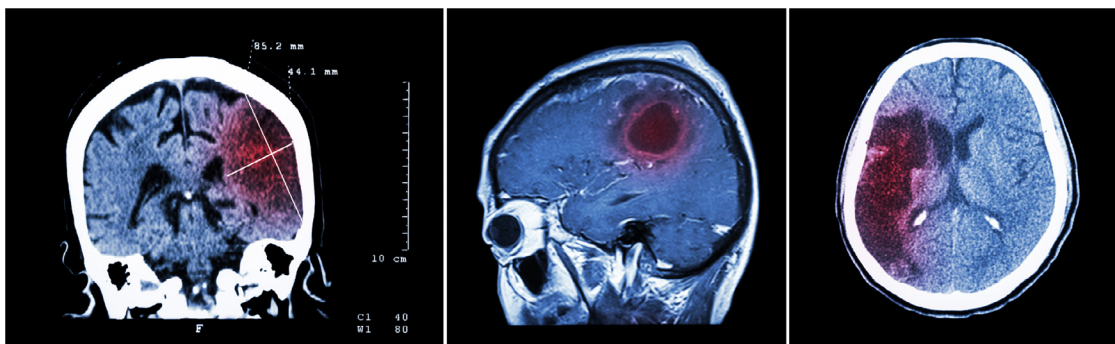


Fig. 1. An MRI for an Ischemic Stroke Case.

estimate of the topological complexity of an object. With its comprehensive characteristic, fractal analysis encompasses some different methods which calculate the fractal dimension of object in a plane [7,8]. The concepts regarding fractal methods enable simple geometrical interpretation required to be used in different realms such as fluid mechanics, geophysics, biology and neurosciences, to name just a few. Fractal method has been extensively used in recent years in data analysis problems in general and particularly in the medical field.

Stroke is among the leading significant reasons for death following cancer and cardiovascular disorders (see Fig. 1). Being a life-threatening neurological disease, stroke is ranked as the third leading reason for death in developing countries and the US [9]. It is characterized by the rapid loss of brain function due to the disturbance occurring in the blood supply and oxygen to the brain [10,11]. Stroke results in cognitive impairment and vascular dementia [4,12]. In addition, it can bring about motor visual and speech problems. Stroke generally may be categorized into two clinical types: the ischemic stroke and hemorrhagic stroke [13].

This study is concerned with the dataset of individuals diagnosed with ischemic stroke: no stroke/TIA, large vessel, small vessel, cardioembolic, cryptogenic, dissection, other (moyamoya, fibromuscular dysplasia (FDM), hereditary, coagulopathy, vasculitis, other rare). These eight subtypes were examined based on TOAST Criteria [4] (For further detailed explanation of subtypes regarding stroke, see [4,14–18]).

Diagnosing and future prediction regarding the development and course of disorders play a critical role. As is the case with all the other disorders, this also holds true for stroke, which proves to be a critical medical concern. At this point, cooperation with medical doctors comes to the fore. In order to assist and enhance diagnosis, prediction and follow-up, numerous methods in diverse fields have been developed so that the life quality of the patients is maintained at a favourable level and enhance that quality further, which requires an interdisciplinary collaboration ultimately with a holistic approach [3,19,20]. Accordingly, there has been a need for practicable techniques and one of such practical methods can be the Box-counting (BC) method, which is one of the multifractal methods. BC is based on the idea of “covering” the image with rectangular coordinate grid [20]. It is considered to be a beneficial method to estimate fractal dimension; therefore, BC is utilized extensively among other fractal techniques [20,21] as an appropriate fractal dimension for the estimation of images that have or do not have self-similarity.

To cite relevant studies related to Box-counting, [22] worked on characterization of stroke lesions with 15 different datasets by using fractal Box-counting analysis. The results of the study offer an efficient scheme to characterize stroke lesions by means of fractal parameters. The study of [23] is concerned with carotid atherosclerotic lesions in cerebrovascular disease with the aim of devel-

oping and validating novel vulnerability biomarkers from three-dimensional ultrasound images (3DUS) using fractal geometry features. Their fractal dimension analysis tool was employed in order to assess the impact of atorvastatin that makes use of 3DUS carotid images. Another study [24] concerned with biomarkers addresses tissue multifractality and Born approximation for precancer detection. The study demonstrates the useful ability of delineation of the multifractal optical properties from light scattering signals for the characterization of an extensive range of non-biological origin. Correspondingly, the study of [25] developed a methodology benefiting from multifractal parameters through the integration of the HMM and support vector machine (SVM) for the optical diagnosis of cancer. The study results demonstrated that the integrated Multifractal Detrended Fluctuation Analysis–Hidden Markov Model attained better discrimination between normal and differing grades of cancer. [26] in their study, had the objective of determining the way to prepare an image for Box-counting analysis. They concluded that determining the most appropriate range of box sizes is encountered as a common problem for any image type and the applications need to be conducted repeatedly for each of the individual images. [27] worked on the different morphological forms where astrocytes occur in brain of Alzheimer’s disease and ischemic/hemorrhagic stroke patients. The authors applied a fractal dimension analysis algorithm to differentiate between astroglia through their analysis of over 1000 astroglia. Their work demonstrates that fractal dimension analysis of astroglia is a beneficial method for describing gliosis quantitatively in different pathologies, which may provide insight into the brain diseases’ pathogenesis.

Wavelet transform (WT) provides certain benefits, one of its remarkable properties is its ability to characterize the local regularity of functions and the local regularity is often measured with Lipschitz exponents (LE) [28]. While locally investigating a fractal function, the Hölder exponent is governed by the singularities, which causes oscillations around the WT amplitude’s expected power-law behavior. In such cases, WTMM method is preferred to be used so that this exact calculation problem can be overcome. This is one advantage of WTMM method. Another major positive aspect of using wavelets is that the wavelet transform modulus-maxima offers an adaptive space-scale partition to extract the singularity spectrum by means of scaling behavior of some partition functions defined on the WTMM [29]. There is further advantage to modulus maxima proven by simulation experiments yielding acceptable results of singularity decisions concerning the noisy signal and achieving better performance [30]. Furthermore, the studies of [31,32] have also proven that WTMM is possible to be utilized for the definition of a multifractal-like formalism and for the determination of many signals’ multifractal nature [33].

WTMM has been used in several studies in the literature over the recent years. The study by [34] concerns machinery health

monitoring as a key step in the maintenance implementation in industry. The study conducted presents that Lipschitz exponent is the most popular measure regarding the regularity behaviour of a signal; and wavelet transform has the ability of characterising the local regularity of machines. As a result of the analysing and diagnosing of measuring vibration signal with the use of LE based objective function, the algorithm they worked on proved to have reliability and effectiveness. In a study performed by [35], in which medical data were used, WTMM approach was employed to study the dynamics of cerebral blood flow (CBF) in rats. The results show that the wavelet-based multifractal formalism ensures the quantifying of essentially different reactions concerning the level of large and small cerebral vessels. The authors put forth the major significance of wavelet-based multifractal formalism, stating that it is likely to be the most powerful tool to do statistical analysis concerning inhomogeneous and nonstationary processes. This particular approach is advantageous owing to its essential potential of quantifying the natural systems' complex dynamics. Another study in engineering was conducted by [36] who analysed the classical pulse superposition method based on wavelet-modulus-maxima information. Their experiments based on practice demonstrated that the method proposed was straightforward and effective, which prove to be noteworthy for engineering applications.

The use of WTMM in natural sciences, industry and engineering is seen in various fields and applications. To illustrate from the recent works, [37]'s work is concerned with time series in solar wind speed. The authors investigated the existence of multifractality within the boundaries of the signal. For this, they employed Continuous wavelet transforms modulus maxima method. The span of the time series data examined is of 2492 days (between 01/01/1997 and 28/10/2003). The authors drew singularity spectrum to assess qualitatively the level of multifractality existent within the solar wind speed signal. Besides the use of WTMM in natural sciences and engineering, its use in medical areas would be worthy of being mentioned [38]'s study also concerns one of the medical issues, cardiac arrhythmia. It is stated by the authors of the study that the wavelet transform is an effective tool to extract discriminative features. The authors proposed an improved algorithm based on multiresolution wavelet transform to classify four types of electrocardiogram (ECG) beats. Their results showed that support vector machine (SVM) approach had a superior classification accuracy for the detection of detecting ECG arrhythmia beats. Concerning classification and artificial neural networks (ANN), [9]'s study is related to stroke by the classification algorithms (Neural Network, Decision Tree and Naive Bayes). They used the methods for the prediction of stroke presence including related number of attributes. In their study, the authors employed the principle component analysis algorithm to reduce the dimensions and they presented the predictions concerning whether the patient is suffering from the stroke disease or not [39] proposed a functional model of ANN to assist the already existing methods of diagnosis. They examined the use of ANN for the prediction of thrombo-embolic stroke disease. The work of the authors shows that the ANN based prediction of stroke disease enhances the accuracy for diagnosis, having attained a higher consistency, which suggests that ANN performance is at a good level for the prediction of stroke in general. Another study on stroke and application of ANN was done by [40] to predict the stroke outcomes through the use of ANN, SVM models and knowledge discovery process methods. Their data included 297 individuals and the findings of the study demonstrated that ANN yielded a higher predictive performance in comparison with SVM for stroke prediction. Finally, the study by [41] presents a development of a Mobile Cloud System (MCC) for stroke subtypes. The dataset was comprised of stroke patients with cardioembolic (689) and cryptogenic (528) subtypes. One of the

ANN algorithms, Multilayer Perceptron Algorithm (MLP), proved to be beneficial for the classification of the two stroke subtypes. The study findings and the proposed healthcare system revealed that the model ensured security and scalability as a system for stroke patients as a result of accurate classification process.

By the same token, fractal and multifractal methods have been applied extensively over the last years in numerous analyses of medical data. Application of this geometry relies heavily on the estimation of the fractal features. Based on this, various methods have been proposed for the estimation of the fractal dimension or multifractal spectral concerning medical data. To cite relevant studies, [4,41,42] did works by selecting the most significant attributes for the early detection of stroke. [11] and [43,44] made the selection of the most significant stroke attributes and performed the application by machine learning algorithms. [44] demonstrated one of the essential potentials of the Wavelet transform modulus maxima approach for the characterization of functional distortions in cerebrovascular dynamics for both small and large vessel.

The approach in this study is more extensive when compared with other studies done with stroke datasets [4,39–44] in the literature. The reason why it is extensive is owing to the dimension of the dataset and the multifarious methods applied. Considering the dimension of 2242 (the number of patients with 8 different stroke subtypes) and 23 attributes, the dataset is comprehensive. The 8 stroke subtypes are no stroke/TIA, large vessel, small vessel, cardioembolic, cryptogenic, multiple coexisting, dissection, other (moyamoya, FMD, hereditary, coagulopathy, vasculitis, other rare). The attributes consist of demographic information, medical history, results of laboratory tests, treatments as well as medications. This extensive data with 8 different stroke types and all the attributes handled in the study naturally fall into the category of big data; and when compared to other relevant studies in the literature, the data handled in this study is highly comprehensive. The big data analysis in this respect is one contribution of the current study. Among the previous researches conducted in this area, there are extant analyses on stroke datasets. However, no work has been reported yet which concerns the aforementioned attributes. Additionally, in terms of method, this study is also the first in the literature since Box-counting dimension (with least square regression) and Wavelet transform modulus maxima (with Gaussian wavelet analysis) have been used for the identification of regular, self-similar, efficient and significant attributes. Methods utilized in the study; therefore, are applicable to the case where the data has irregular and differentiable features with fractal structures. Regarding the methods used, the methods comprise a second contribution of this study. The method provides two approaches. As the first approach, in terms of identifying the significant, efficient, self-similar and regular attributes, the methods used facilitated the classification. Therefore, fractal and multifractal methods, BC and WTMM, were applied to identify the discriminating and significant singular attributes to diagnose stroke subtypes. To attain this aim, the first step was to identify the significant, self-similar and regular attributes. For this, the Box-counting dimension (with least square regression) was applied on the stroke dataset (see Tables 1 and 2 for further details). Thus, the new dataset was obtained (BC_stroke dataset). As the second step, the significant, self-similar and regular attributes were identified by the Wavelet transform modulus maxima (with Gaussian wavelet analysis) application. The new dataset was obtained accordingly (WTMM_stroke dataset). As the second approach of the method, FFBP algorithm, one of the ANN algorithms, was applied on the stroke dataset, BC_stroke dataset as well as WTMM_stroke dataset for the classification of stroke subtypes. The classification by FFBP algorithm enabled the calculation of overall accuracies based on sensitivity, specificity, accuracy rates. Based on these elements, the accuracy rates of the three datasets

Table 1
Breakdown of stroke dataset attributes.

Number of Stroke Subtypes/TOAST	Main Headings of Attributes	Data Size
No Stroke /TIA (167)	Demographic information (Age, Gender)	2242x23
Large Vessel (481)	Medical history (HTN, hyperlip, DM, H/O Stroke/TIA, AtrialFib,	
Small Vessel (228)	CAD, CHF, PAD/Carotid disease, tobacco, ETOH)	
Cardioembolic (689)	Results of laboratory test (mRS 90 days, hemorrhagic conversion, NIHSS admission, TPA)	
Cryptogenic (528)	Treatment and medication data (Statin, antiHTN, antidiabetic, anticoagulation, CT perfusion, neurointervention)	
Multiple Coexisting (38)		
Dissection (59)		
Other (52)		

TOAST: type/etiology of stroke; TIA: ischemic attack; HTN: hypertension; DM: diabetes mellitus; CAD: coronary artery disease; AtrialFib: atrial fibrillation stroke; CAD: coronary artery disease; CHF: congestive heart failure; PAD/carotid disease: peripheral artery disease; NIHSS 90 days: National Institutes of Health Stroke Scale 90-day mortality; CT perfusion: computer tomography perfusion; ETOH: alcohol; antiHTN: antihypertensive drugs after acute ischemic stroke; NIHSS discharge: National Institutes of Health Stroke Scale; H/O stroke/TIA: history of transient ischemic attack.

Table 3
The stages of the proposed approach.

```

Input : stroke dataset = [2242 × 23]
Place the stroke subtypes as target data into a matrix O[8 × 1]

Stage 1. stroke dataset
Stage 2. stroke dataset applied to Box Dimension as 1-D attributes
Estimate log(N(r))/log(r) (r= 1 to 2242)
Obtained (BC_stroke dataset = [2242 × 12])
Apply FFBP algorithm on the BC_stroke dataset = [2242 × 12]
for the classification of stroke subtypes
Stage 2. stroke dataset applied to WTMM method as 1-D attributes
Applied Gaussian wavelet as 1-D
Obtained (WTMM_stroke dataset = [2242 × 12])
Apply FFBP algorithm on the WTMM_stroke dataset = [2242 × 12]
for the classification of stroke subtypes
Stage 3. FFBP Classification 5 × 5 cross validation
Divide input data (stroke_dataset = [2242 × 23],
BC_stroke dataset = [2242 × 12], WTMM_stroke dataset = [2242 × 12])
randomly for 70% training, 15% test,
15% validation and target data O[8 × 1] into 5 different folds.
for j = 1.5
Use the j = th fold for test, and the rest two folds are merged
as the training set.
Record the classification results over jth fold.
end
Output:
Make the sum of the classification results over each fold
for the subtypes of stroke
Report overall accuracy
    
```

were compared with one another. Therefore, the most significant attributes were revealed as a result of these applications and calculations.

In that regard, the study is novel and can contribute to the literature by abridging the gap with its big data analysis on stroke subtypes and the multistage methods employed (see Table 3).

1.1. Motivations of the proposed method

The originality of this study is due to the fact that no study exists in the literature in which BC andWTMM methods have been employed. Besides this, it is the first time these methods have been employed on such an extensive stroke data (2242 × 23) for the detection of the singularities in the stroke datasets. The sin-

Table 2
Description of the stroke dataset.

Attributes	Stats	Number of Patients/ Values (%)	Descriptions
HTN	Yes	1593 (72%)	Hypertension
Hyperlip	Yes	1197 (54%)	High levels of lipid (fat) in blood
DM	Yes	602 (27%)	Diabetes
H/Stroke/TIA	Yes	546 (25%)	History of Stroke/TIA
AtrialFib	Yes	541 (25%)	Abnormal heart rhythm
CAD	Yes	513 (23%)	Coronary Artery Disease
CHF	Yes	229 (10%)	Congestive Heart Failure
PAD/Carotid disease	Yes	318 (14%)	Peripheral Artery Disease
Tobacco	Yes	520 (23%)	Cigarette addict
ETOH	Yes	308 (1.7%)	Alcohol addict
Statin	Yes	1000 (45%)	Medications given to the patient are grouped into five broad categories
AntiHTN	Yes	1332 (60%)	
Antidiabetic	Yes	454 (20%)	
Antiplatelet	Yes	1031 (47%)	
Anticoagulation	Yes	242 (10%)	
CT Perfusion	Yes	137 (0.06%)	Procedures used for treatment
NeuroIntervention	Yes	271 (12%)	Dichotomized into Low (0-2) High (3-6)
mRS 90 Days	Low	2007	
	High	197	Whether the ischemic stroke turned to hemorrhagic
Haemorrhagic con.	Yes	204 (0.09%)	
NIHSS admission		9.3+/-8.3	Measures the severity of stroke
TPA	Yes	413 (19%)	TPA (Tissue Plasminogen Activator) is used to break down blood clots

gularity spectrum provides a value concerning how fractal a set of points are in the BC_stroke dataset (2242×12) and WTMM_stroke dataset (2242×12). With the application of multifractal and multifractional BC and WTMM methods on the stroke dataset (2242×23), the two datasets, namely BC_stroke dataset and WTMM_stroke dataset, have been obtained. The comparative analyses have been performed with FFBP, which one of the ANN algorithms. With this integrated multifarious methodology, this present study differs from the earlier ones which employed standard approaches.

Wavelet transform maxima modulus method has provided higher results in the study since the Wavelet transform which utilizes the Wavelet transform maxima modulus method (wavelet based method of multifractal analysis for the detection of the singularities in the stroke datasets) proves to be a highly efficient and novel approach to provide the significant attributes of multifractal content. Besides this, it has also ensured an efficient and reliable way in order to detect the singularities.

Stroke concerns brain which is an intriguing complex structure within a complex system. The complexity of the brain requires sophisticated means and interventions to comprehend its structure and dynamics. Within this framework, complexity analysis enables to understand the structure and function of the brain as a complex system. Problems concerning complex systems tend to be multidimensional, dynamic, nonlinear, non-differentiable and chaotic. In this regard, through such a multifarious approach used in this study, it could be possible to establish innovative systems and provide global optimal solutions in the relevant field both for stroke and other life-threatening medical problems. All such innovative solutions will definitely serve to improve diagnostic processes, treatment courses and ultimately the life quality of the patients.

Considering all these novel aspects and complexity analysis, the study aims at pointing a new frontier in the relevant fields, including modern neurosciences, concerning the complex dynamic systems and structures which display multifractional content.

The paper is organized as follows: Section 2 provides Data and Methodology. Methods of the approach include BC and WTMM, followed by Numerical Experiments (stroke dataset experiments on BC and WTMM methods) and explanation of the Artificial Neural Network Algorithm (FFBP). As the last sections, Experimental Results, Discussion and Conclusion and Limitations are presented in Sections 3, 4 and 5, respectively.

2. Data and method

2.1. Data

The dataset is made up of 2242 individuals who had been taken under observation at Massachusetts Medical School University of Worcester, Massachusetts, USA and were diagnosed with absolute clinic stroke subtypes. The study has been ethically approved by University of Massachusetts Medical School and Stroke Services at UMass Memorial Medical Center. Data for stroke dataset were collected between March 9, 2007 and October 2, 2016. The total 2242 Ischemic stroke (see Fig. 1) subtypes include No Stroke/TIA (167), Large Vessel (481), Small Vessel (228), Cardioembolic (689), Cryptogenic (528), Multiple Coexisting (38), Dissection (59), Others (moyamoya, FMD, hereditary, coagulopathy, vasculitis, other rare) (52). Fig. 1 depicts an example MRI of an ischemic stroke case.

A total of 2242 patients were included in the applications. Ischemic stroke patients, aged between 0 and 104 (see Table 1), with eight subtypes of ischemic stroke were taken under examination in this study. The ischemic strokes in the dominant hemisphere lead to more functional deficits compared to the strokes in the non-

dominant hemisphere as they are evaluated on the National Institutes of Health Stroke Scale (NIHSS).

Table 1 provides the main headings of attributes that are demographic information, medical history, results of laboratory tests, treatments and medication data, (see further details in [4,11–18,41]) handled for the stroke subtypes.

The patients' baseline characteristics as stratified by infarct side are summarized in Table 2.

2.2. Methodology

This study presents the contributions in two approaches. Based on this, the aim of the paper is to determine the self-similar, regular, significant and efficient attributes to achieve high rates of accuracy classification for stroke subtypes which are No Stroke/TIA, Large Vessel, Small Vessel, Cardioembolic, Multiple coexisting, Cryptogenic, Dissection, Other (moyamoya, FMD, hereditary, coagulopathy, vasculitis, other rare). The steps in this study can be indicated in the following way:

The first approach is the application of Box-counting dimension and Wavelet transform modulus maxima which are two of the fractal and multifractal methods. The steps for the application of this approach are provided in detail below:

(a) Box-counting dimension (with least square regression) was applied on the stroke dataset in order to identify the regular, self-similar, efficient and significant attributes from the stroke dataset. In this way, the dataset named BC_stroke dataset was generated.

(b) Wavelet transform modulus maxima (with Gaussian wavelet analysis) was applied on the stroke dataset in order to identify the regular, self-similar, efficient and significant attributes from the dataset. Thus, the dataset WTMM_stroke dataset was generated.

The second approach of the study involves the application of Feed Forward Back Propagation (FFBP), which is one of the ANN algorithms. The steps for this application are as follows: i) FFBP algorithm was applied on the stroke dataset, BC_stroke dataset as well as WTMM_stroke dataset. ii) FFBP algorithm was used for the classification of stroke subtypes. The classification ensured the calculation of overall accuracies based on sensitivity, specificity, accuracy rates; hence, comparative analyses were performed in terms of accuracy rates. iii) By following the steps mentioned above, the attributes which have proven to be most effective for the stroke subtype classification were based on the results with regard to sensitivity, specificity and accuracy rates.

Computations and figures for this study were performed on Matlab [45] and Fraclab [46].

2.2.1. Fractal analysis

A "fractal" designates a fragmented or rough geometric shape which may be divided into subparts each of which is (at least approximately) a reduced size copy of the whole thing [47]. The interpretation of medical data for diagnosis is a task with multiple steps. The purpose is to detect the potential abnormalities. For this purpose, the clinician makes use of the integration of two processes, the first process involves data perception to identify the unique data patterns, the second process involves the detection of the relationship between perceived patterns and potential diagnoses. The achievement of the two processes is mainly dependent on the skill of the clinician at work. Texture, as rich visual source and a major element in image analysis, is one of the utilized features [48].

2.2.2. Fractal dimension

Fractal frequently comes to the fore with regard to the evaluation of the fractal dimension (named as FD or D). FD is considered to be a useful concept for the description of natural objects, indicating their degree of complexity. Mandelbrot (1983) introduced

the term to reflect objects which have complex geometry and that kind of geometry cannot be characterized by an integral dimension [21].

In order to compute this dimension, several methods with their own theoretical basis are applicable, and it is due to this fact that enables one to obtain different dimensions for the same feature through different methods. The difference may be observed since the Hausdorff-Besicovitch dimension Eq. (1) is not computable in this form in majority of the cases [48–51].

$$D_h = \frac{\ln(N)}{\ln\left(\frac{1}{r}\right)} \quad (1)$$

The homothety term may be linked with a reduction term. For instance, a fractal according to Eq. (1) is made up of patterns whose size has been reduced of a factor (for homothety). Hence, the methods approximate it with the use of several different algorithms for the estimation of parameter. Despite the differing applied algorithms, they comply with the same basis which can be outlined in the following three steps [21]:

- The quantities of the object are measured by utilizing different step sizes.
- Log (measured quantities) is plotted versus log (step sizes) and
- A least-squares regression line is fitted throughout the data points.

FD needs to be estimated as the slope of the regression line. Data are represented on a finite scale grid in Box-counting methods, and the grid effects interact with computing fractal dimension.

2.2.3. Box-counting method

As one of the most frequently used methods for the FD calculation, the Box-counting method was defined by Russell *et al.* (1980) [6,21]. In Box-counting approach, the curve is covered with a collection of square boxes. The number of elements for a given size is counted so that how many of them are necessary to cover the curve completely can be seen. When the size of the area element comes closer to zero, the total area covered by the area elements converges to the measure of the curve [52,53]. The FD is estimated as Eq. (2) covering a binary data with the boxes of length r ,

$$FD = -\lim_{r \rightarrow 0} \frac{\log(N(r))}{\log(r)} \quad (2)$$

Here, $N(r)$ refers to the number of boxes which are required to cover the data completely. Since this method needs data binarization, it comes with many limitations. For instance, the method is not well established in terms of theoretic foundation, and it is valid merely for statistically self-similar data. Besides this, the grid needs to be relocated randomly at each iteration since the reiteration for different sizes of r may yield different sizes of N_r .

In the present study, the Box-counting method, whose aim is to consider the average number, notes $N(r)$ of boxes with a fixed side length r , which is required to cover the data. Therefore, the estimation of $P(m, r)$, the probability that one box of size r , is done, which is centred on arbitrary point of data, including m points of the set Eq. (3) shows this situation: [52,53]

$$\forall r, \sum_{m=1}^{N_p} P(m, r) = 1 \quad (3)$$

Here, N_p refers to the number of possible points in the R^3 which refers to space. The estimation of the average number of disjointed boxes required to cover the surface is denoted as in Eq. (4).

$$N(r) = \sum_{m=1}^{N_p} N(m, r) = \sum_{m=1}^{N_p} \frac{P(m, r)}{m} \quad (4)$$

The estimation through the least squares method of the group of dots' slope ($\log(r)$), $-\log(N(r))$, obtained by the boxes of increasing size r , yields the fractal dimension for stroke dataset (with 23 attributes). The Algorithm 1 [54–56] provides this calculation as Algorithm 1.

Algorithm 1 The Box-counting method Algorithm.

```

for  $r=1$  to  $r_{\max}$  and  $m=1$  to  $r$ 
 $P(m,r)=0$ 
for any site  $s$  of the stroke dataset (23 attributes){
for  $r=1$  to {
Center a 1-D  $r$  on  $[s, A[s]]$ 
Count the number  $m$  of data of the stroke
dataset which belongs to the  $r$ 
Increment  $P(m,r)$  of 1
}
}
for  $r=1$  to  $r_{\max}$ 
 $N(r) = \sum_{m=1}^{N_p} \frac{P(m,r)}{m}$ 
Estimate by the method of least squares the slope
 $D$  of the curve ( $\log(r)$ ,  $-\log(N(r))$ )

```

2.2.4. Multifractal analysis

Multifractals can be regarded as an extension of fractals. An object that is multifractal is more complex since it is all the time invariant by translation even though the dilatation factor required to distinguish the detail from the whole object is reliant on the detail that is being observed. Regarding the FD estimation, many methods are applicable to make the approximation of the multifractal spectrum as wavelets [51–58].

2.2.5. Wavelet transform

Ψ be a real function, which is said to be a wavelet if its integral is zero as Eq. (5) [28,56].

$$\int_{-\infty}^{\infty} \Psi(x) dx = 0 \quad (5)$$

The continuous wavelet transform of a function $f \in L^2(R)$ for the wavelet Ψ is defined in Eq. (6).

$$Wf(u, s) = \int_{-\infty}^{\infty} f(t) \frac{1}{\sqrt{s}} \Psi^* \left(\frac{t-u}{s} \right) dt \quad (6)$$

Here Ψ^* refers to the complex conjugate of Ψ .

A wavelet $\Psi(x)$ is stated to contain n vanishing moments if and only if for all positive integers $k < n$, it fulfills Eq. (7) [28,56].

$$\int_{-\infty}^{\infty} x^k \Psi(x) dx = 0 \quad (7)$$

A wavelet frequently applied is the n th derivation of the Gaussian function, and is indicated in Eq. (8).

$$\Psi_n(x) = -\frac{d^n}{dx^n} e^{-\frac{x^2}{2}} \quad (8)$$

The number of vanishing moments is significant while conducting the wavelet singularity analysis since it gives an upper bound measurement for the singularity characterization [28,58–60].

2.2.6. Singular exponent

A function $f(x)$ is noted to be Lipschitz α , for $0 \leq \alpha \leq 1$, at a point x_0 , provided that a constant A such that for all points x in a neighborhood of x_0 exists Eq. (9) [28,60].

$$|f(x) - f(x_0)| \leq A|x - x_0|^\alpha \tag{9}$$

The function $f(x)$ is Lipschitz α for any $x_0 \in (a, b)$ and $x \in (a, b)$ in a uniform way. It is stated that $f(x)$ is singular in x_0 if it is not Lipschitz 1 in x_0 . If a function is Lipschitz α , for $\alpha > 0$, it is continuous in x_0 [60]. On the other hand, if $f(x)$ is discontinuous in x_0 and bounded in a neighborhood of x_0 , it is then Lipschitz 0 in x_0 . If $f(x)$ is continuously differentiable, then it is Lipschitz 1 and hence it will not be singular. It is assumed that the $\Psi(t)$ owns a compact support, is n times continuously differentiable and is the n th derivatives concerning a smoothing function [60].

2.2.7. The detection of singularity with wavelet

The detection of singularity with wavelet is a measurement of a singularity's strength. When the theorems used in this study are examined, it is important to note that Jaffard (1991) [61] made the generalization of Mallat's Theorem to pointwise Lipschitz regularity. Mallat's Theorem is considered to be an outcome of Jaffard's Theorem (Jaffard, 1989 [62]; Farge, et al., 1993 [63]). In this regard, Jaffard's Theorem presents a sufficient condition on the modulus of the Wavelet transform to compute the Lipschitz regularity of $x(t)$ at point τ . Accordingly, as shown by Mallat et al. [58], it is possible to compute by the WTMM of the data. Some relevant definitions on this may be found [50,60,63], below:

Local maxima of wavelet transform modulus $Wf(u)$ is the wavelet transform of a function $f(u)$ [28,50,58].

- A local maximum is the point u_0, s_0 in that $\frac{\partial Wf(u, s_0)}{\partial u}$ has a zero-crossing at $u = u_0$, when u changes.
- A modulus maximum is the point u_0, s_0 where $|Wf(u, s_0)| < |Wf(u_0, s_0)|$ when u goes either to right or left neighborhood of u_0 and $|Wf(u, s_0)| \leq |Wf(u_0, s_0)|$ when u goes to the opposite neighborhood of u_0 .
- A maxima line calls any linked curve in the scale space (u, s) throughout which all points are modulus maxima.

We assume that the Ψ owns a compact support, with n times being continuously differentiable, and is the n th derivative for a smoothing function.

Theorem 1: f is a tempered distribution and its wavelet transform is defined well over (a, b) . Moreover, let $u_0 \in (a, b)$. It is assumed there is a constant C and scale $s_0 > 0$, in addition to this, for $u \in (a, b)$ as well as $s < s_0$, all the modulus maxima of $|Wf(u, s)|$ belong to a cone whose definition has been provided in Eq. (9) [28,58,62].

$$|u - u_0| < Cs \tag{10}$$

In this case, $u_1 \in (a, b)$, $u_1 \neq u_0$, f is uniformly Lipschitz α at u_0 at all points, and provided that at each modulus maxima (u, s) in the cone, there is a constant A , whose definition is in Eq. (10) [28,31,64–69].

$$|Wf(u, s)| \leq As^\alpha \tag{11}$$

This theorem is the mathematical base for the estimation of LE [28,58,59,65].

By the substitution of the S_i and S_{i+1} into Eq. (11) with simple derivation, Lipschitz exponents can be stated in the following way [28,58,59]:

$$\alpha = \frac{\log_2 \left| \frac{Wf(s(i+1)X)}{Wf(s_i X)} \right|}{\log_2 \left| \frac{S(i+1)}{s_i} \right|} \tag{12}$$

The value of Lipschitz exponent α can reflect the degree of failure. If the Lipschitz exponent is smaller, then the curve deviates will be stronger.

2.2.8. Lipschitz exponent measuring with WTMM

Based on the Theorem 1, the Lipschitz exponent can be measured by employing Algorithm 2 indicated below [28,50]:

Algorithm 2 LE Measuring with WTMM.

-
- Step 1. Calculate the straight line $l(\log_2(s))$ that links both $(\log_2(s_{small})$ and $\log_2|Wf(u, s_{small})|)$ and $(\log_2(s)_{max}$ $\log_2|Wf(u, s_{max})|)$.
 If $l(\log_2(s)) \geq \log_2|Wf(u, s)|$ return the intercept $\log_2(A)$ and slope α of $l(\log_2(s))$, go along with step 6, if not, go along with step 2.
 Step 2. Let $s = s_{max}$ and $f(A, \alpha) = C$ where C is a constant that is large enough.
 Step 3. Compute tangent $l(\log_2(s))$ at $\log_2(s)$, $\log_2|Wf(u, s)|$. If $l(\log_2(s)) \geq \log_2|Wf(u, s)|$ go along with Step 4.
 If not, continue with Step 6.
 Step 4. Compute record of the result f and intercept $\log_2(A)$ and slope α of $l(\log_2(s))$.
 If $f < f(A, \alpha)$, $f(A, \alpha) = f$ and $LE = \alpha$.
 If $s = s_{min}$, continue with Step 6, if not, continue with Step 5.
 Step 5. $s = s - \Delta \log_2(s)$, go along with Step 3.
 Step 6. Output $LE = \alpha$
-

Since a priori knowledge of α is used, and the algorithm looks for the optimal result along $\log_2|Wf(u, s)|$ curve only. The problem of initialization of A and α can be prevented [31,50,58,65].

2.3. Numerical experiments

Results regarding the stroke dataset are presented and in all of the cases, the outcome of the Box-counting dimension and Wavelet transform modulus maxima methods is presented. Regarding the procedures for stroke dataset, the attributes (see Table 1 and Table 2) are set so that the best fit to the known original data can be obtained. An extensive range of sampled functions of 2242 length are handled for the estimate of local regularity for each of the 23 stroke attributes (see Table 1). In this study, numerical experiments were obtained by BC and WTMM methods, which were applied to numerical experiments concerning the stroke dataset (see Table 2). The fractal method and multifractal method were applied on the stroke dataset in order to attain the significant, self-similar and regular stroke datasets (BC_stroke dataset, WTMM_stroke dataset). The following steps were followed for this purpose:

Step 1: The brutal fall of the number of boxes after the side length $r = 1$ is considered, which explains the existence of a significant number of boxes 1-dimension for the attributes of stroke dataset.

Step 2: For the capturing of pointwise LE, the maxima seem to be sufficient while analysing regularity with Wavelet transform Modulus Maxima (WTMM). The detection of singularity is computed by the LE Measuring with WTMM.

In this study, fractal method (the Box-counting dimension) (with least square regression) and multifractal method Wavelet transform modulus maxima (with Gaussian wavelet analysis) are applied to identify the self-similar, efficient and significant attributes (see Table 2) in the stroke subtypes. Stroke dataset, BC_stroke dataset and regular WTMM_stroke dataset (BC_stroke dataset and WTMM_stroke dataset are made up of significant attributes) were classified with the FFBP algorithm. As a result of the steps, WTMM yielded the most accurate results for the classification of the 8 subtypes of stroke based on sensitivity, specificity and accuracy rate.

2.4. Artificial neural network algorithm

Neural networks are constructed based on simple units which are linked with one another by a set of weighted connections. In general, these units have their organization in the form of layers. Every unit of the first layer, namely the input layer, refers to a feature of a pattern which will be taken under analysis. The units concerning the last layer, namely the output layer, yields a decision following the information propagation. Accordingly, artificial neural networks (ANNs), or systems that are known to be connectionist, are computational systems that have been inspired by biological neural networks which imitate animal brains. The procedure utilized to perform the learning process in a neural network is named as the training algorithm. Feed Forward Back Propagation algorithm is one of the ANN algorithms.

2.4.1. Feed forward back propagation algorithm

As one of the most frequently-used artificial neural networks, feedforward neural network is an artificial neural network within connections between the units which do not constitute a cycle [6]. In this regard, it differs from the recurrent neural networks. The feedforward neural network is known to be the first and simplest type of artificial neural network that has been devised. Information moves only in one direction forward from the input nodes through the hidden nodes (if there is any) and to the output nodes. No cycles or loops exist in the network [6].

The network architecture of the algorithm is defined and the weights are involved [6,70]. When the input examples with m -dimension is entered, $x_i = [x_1, x_2, \dots, x_m]^T$ can be seen. Similarly, the output examples for n -dimension is stated by $d_k = [d_1, d_2, \dots, d_n]^T$ (see Fig. 2). x_i values, the output values of the neurons in the i th layer (n), the total input that will correspond to a neuron in j layer is administered in line with the equation (13) [6,70–72] (see Fig. 2).

$$net_j = \sum_{i=1}^m w_{ij}x_i \quad (13)$$

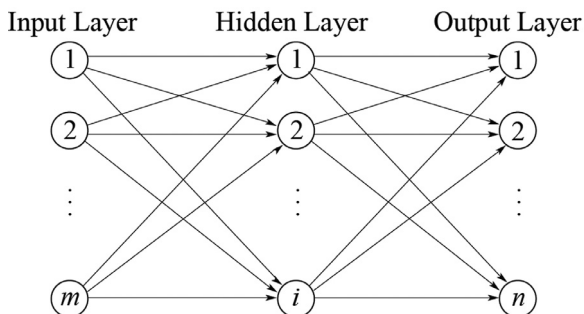


Fig. 2. FFBP algorithm general network structure.

The output of the j neuron in the hidden layer (transfer function output) is computed as indicated in Eq. (14) [6].

$$y_j = f_j(net_j) \quad j = 1, 2, \dots, J \quad (14)$$

The total input that will correspond to k neuron in the output layer is computed based on Eq. (15).

$$net_k = \sum_{j=1}^J w_{kj} \cdot y_j \quad (15)$$

The computation of the non-linear output of a k neuron in the output layer is conducted in line with Eq. (16).

$$o_k = f_k(net_k), \quad k = 1, 2, \dots, n \quad (16)$$

The comparison of the output obtained from the network and the actual output is done, and based on this, e_k error is calculated [17] [6,70–72].

$$e_k = (d_k - o_k) \quad (17)$$

d_k and o_k signify the target of any k neuron in the output layer and the outputs obtained from the network, respectively. The weights obtained from the output layer are also updated. The calculation of the total square error is performed as in Eq. (18) for each example [70–72],

$$E = \frac{1}{2} \sum_k (d_k - o_k)^2 \quad (18)$$

In this study, FFBP algorithm was applied to the three datasets, which are stroke dataset (2242×23), BC_stroke dataset (2242×12) and WTMM_stroke dataset (2242×12), to classify the subtypes of stroke.

3. Experimental results and discussion

This section of study has four main parts: 3.1 deals with the BC dimension the application of the BC method on the stroke dataset (in which least square regression, 1-D was used). 3.2 concerns the application of the WTMM method on the stroke dataset with LE Measuring (in which the Gaussian wavelet analysis was employed) and 3.3. addresses the Application of the FFBP algorithm on the stroke datasets. 3.4 presents the classification results of the stroke datasets with the FFBP algorithm.

Two different approaches were employed in this study. As the first approach, BC method, one of the fractal methods, and WTMM method which is one of the multifractal methods, were utilized. And for the second approach, FFBP algorithm, which is one of the ANN algorithms, was used.

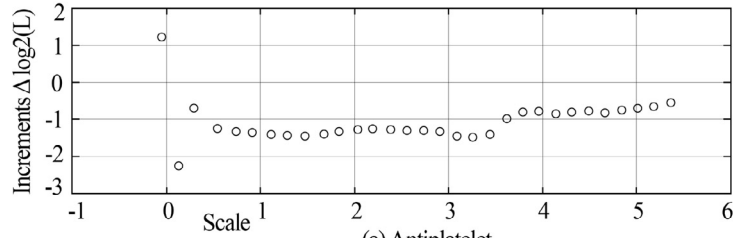
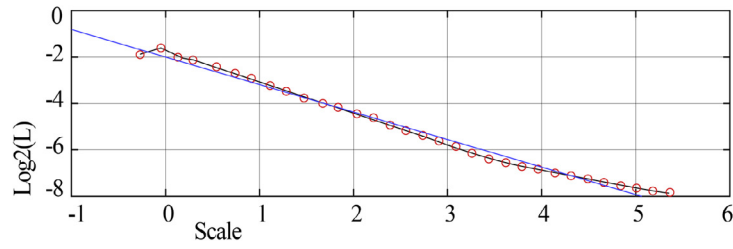
Table 2 provides the multi stages for the application of these two approaches in detail:

The stages for application as presented in (Table 3) are presented in the further sections (3.1., 3.2, 3.3. and 3.4).

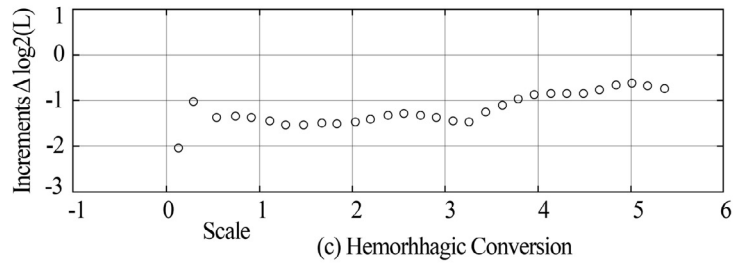
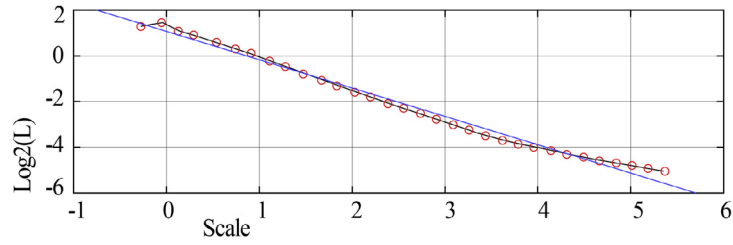
3.1. Application of the box-counting method on the stroke dataset

The attributes of the significant stroke dataset (with 23 attributes) are detected by fractal dimension. The dimension of the stroke dataset is (2242×1). Fig. 3–6 provide the results of the calculation of fractal dimension. Plot curves show the number of boxes in comparison with their side length r . The straight regression line estimates possible $\log(N(r))$ versus $\log(r)$, and the plot is to be performed on all the points, outdistancing it between the size of boxes (equaling to 1) [56]. Fig. 4 indicates the number of boxes based on their sizes (r), in this case $r = 1$ to 2242. It is noticed that the smaller the size is, the larger the number of boxes is. Similarly, the more the size of the boxes is increased, the more the number of them approaches 0. Besides these, the brutal decline in

Estimated Regularization Dimension = 2.19 Corr Coeff: -1 MaxErr/Amplitude : 7.6%



Estimated Regularization Dimension = 2.24 Corr Coeff: -1 MaxErr/Amplitude : 7.9%



Estimated Regularization Dimension = 2.27 Corr Coeff: -1 MaxErr/Amplitude : 8.3%

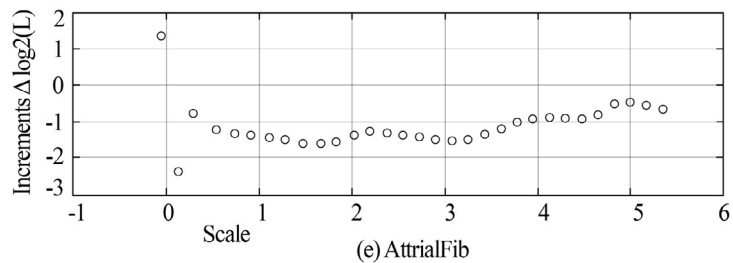
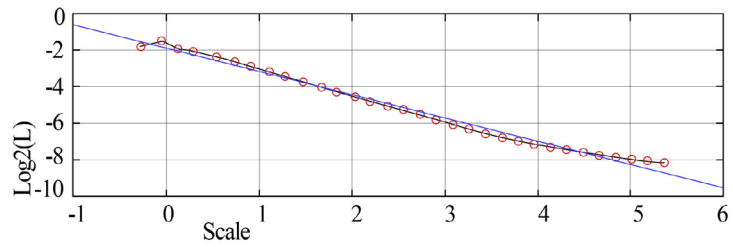
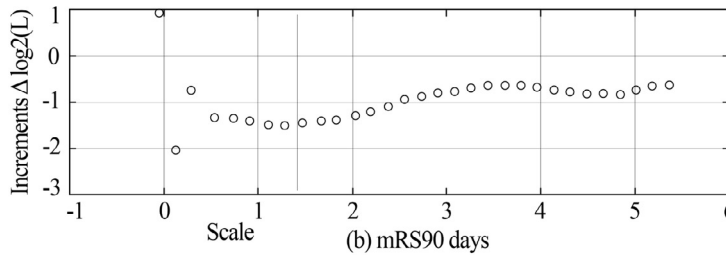
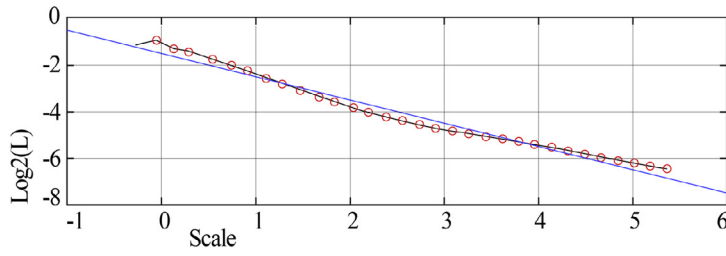
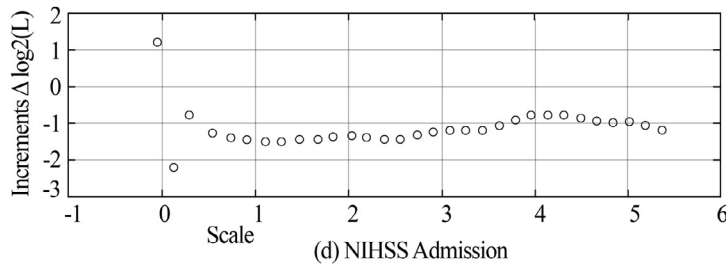
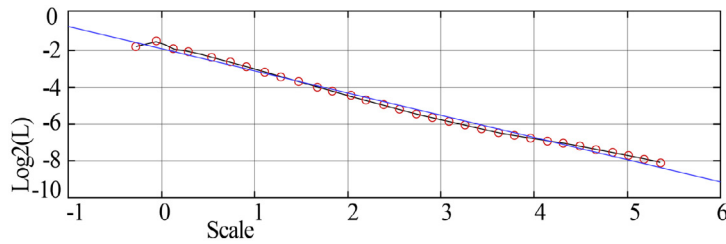


Fig. 3. The plot regression of the curve versus by the least squares method.

Estimated Regularization Dimension = 2 Corr Coeff: -1 MaxErr/Amplitude : 9.1%



Estimated Regularization Dimension = 2.21 Corr Coeff: -1 MaxErr/Amplitude : 5.1%



Estimated Regularization Dimension = 2.26 Corr Coeff: -1 MaxErr/Amplitude : 5.1%

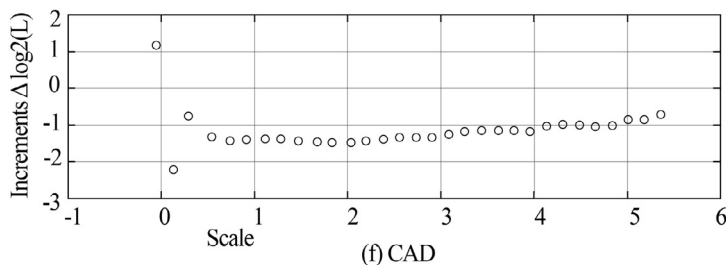
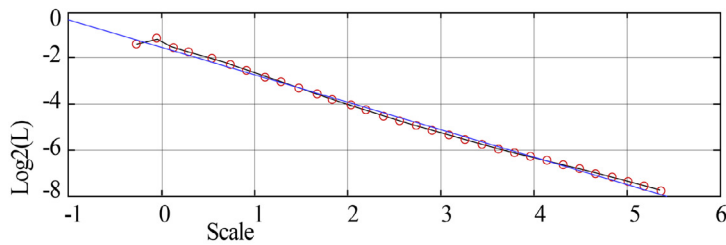
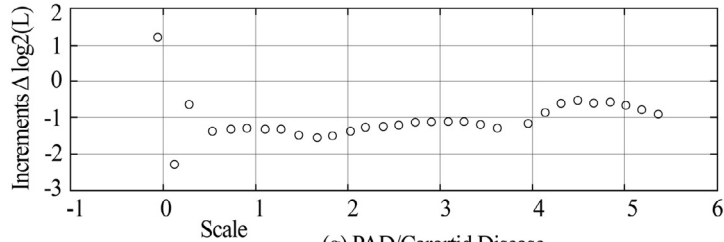
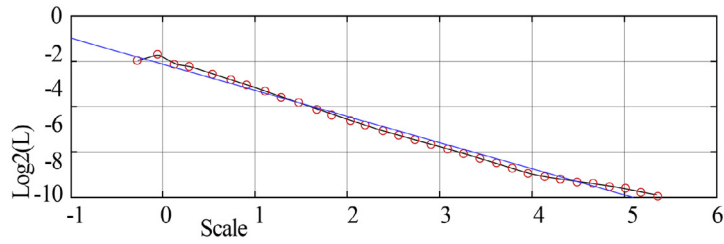


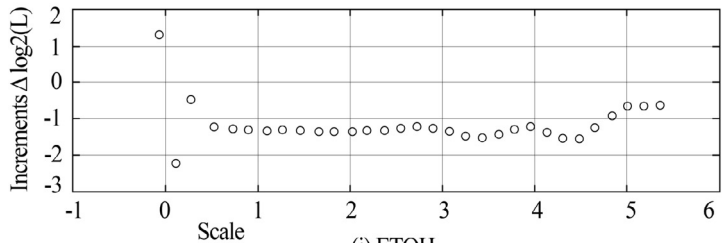
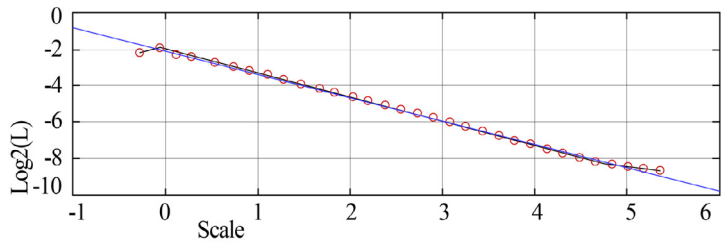
Fig. 4. (Fig. 3 Cont.) The plot regression of the curve versus by the least squares method.

Estimated Regularization Dimension = 2.16 Corr Coe ff: -1 MaxErr/Amplitude : 6.9%



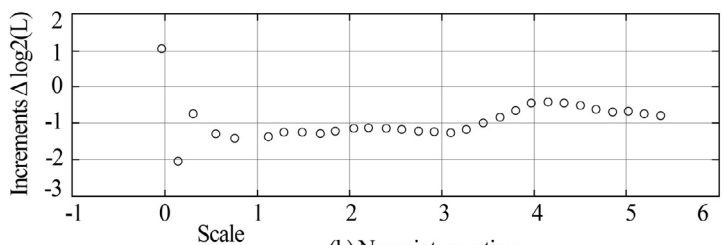
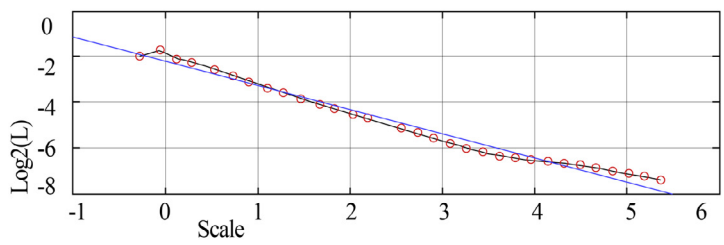
(g) PAD/Carotid Disease

Estimated Regularization Dimension = 2.28 Corr Coeff: -1 MaxErr/Amplitude : 6.9%



(i) ETOH

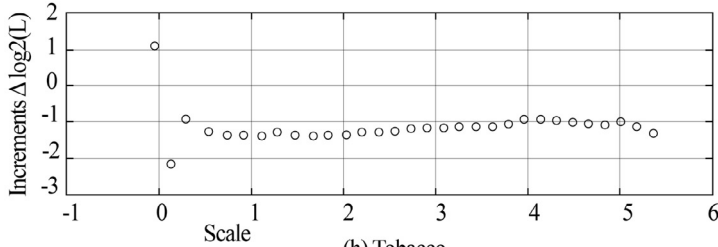
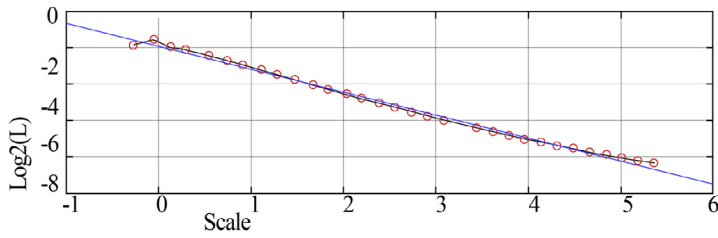
Estimated Regularization Dimension = 2.04 Corr Coeff: -1 MaxErr/Amplitude : 8%



(k) Neurointervention

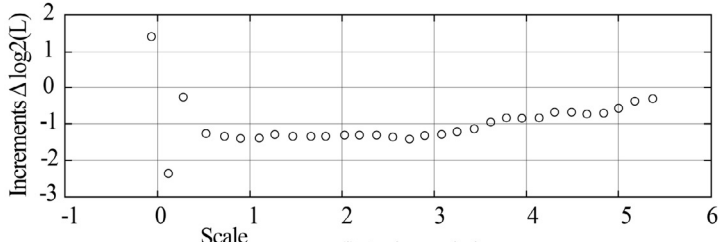
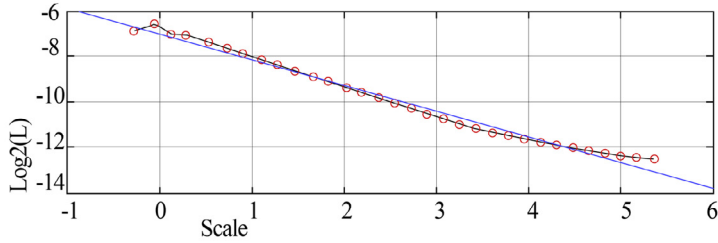
Fig. 5. (Fig. 3 Cont.) The plot regression of the curve versus by the least squares method.

Estimated Regularization Dimension = 2.19 Corr Coeff: -1 MaxErr/Amplitude : 4.9%



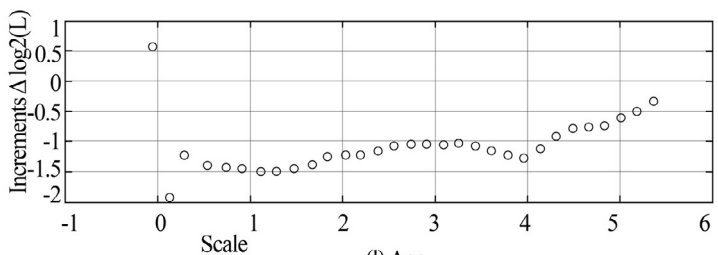
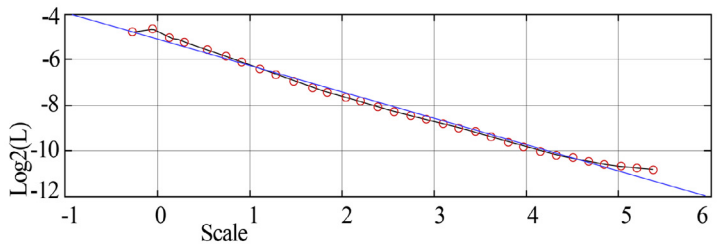
(h) Tobacco

Estimated Regularization Dimension = 2.13 Corr Coeff: -1 MaxErr/Amplitude : 9.5%



(j) Anticoagulation

Estimated Regularization Dimension = 2.16 Corr Coeff: -1 MaxErr/Amplitude : 7.9%



(l) Age

Fig. 6. (Fig. 3 Cont.) The plot regression of the curve versus by the least squares method.

Table 4
Box Dimension results for the stroke dataset at-tributes.

Attributes	Box dimension (D)
Gender	0.89546
Hyperlip	0.95389
DM	0.92445
H/O Stroke/ TIA	0.85709
AttrialFib	0.85048
CAD	0.85668
CHF	0.92449
PAD / Carortid Disease	0.84108
Tobacco	0.8488
ETOH	0.82768
Statin	0.99744
AntiHTN	0.8644
Antidiabetic	0.93629
Antiplatelet	0.80829
Anticoagulation	0.81818

the number of boxes following the side length $r = 1$, explains the existence of a significant number of boxes dimension for the at-tributes of the stroke dataset (for $D < 0.86$) (see Table 4).

As can be seen from Table 4, there is a variability of the values of box dimension. A compromise between r_{min} and r_{max} is always to be taken and these two parameters have impact on one another and also particularly on the FD calculation. For the choice of r_{min} and r_{max} following several tests, it can be stated that it is chosen from 2, which is to have a probability of finding at least one box (for $D < 0.86$). Table 4 presents the Box Dimension results of the stroke dataset based on D.

In this study, the BC method was employed since it is convenient and automatically computable as well as applicable for pat-terns which have or do not have self-similar attributes.

As a result of the Box-counting application on the stroke dataset, the significant, efficient, self-similar and regular attributes were identified. BC_stroke dataset was obtained from this application. The attributes identified are: Antiplatelet, mRS90 days, Hemorrhagic Conversion, NIHSS Admission, AttrialFib, CAD, PAD / Carortid Disease, Tobacco, ETOH, Anticoagulation, Neurointervention, Age (see Table 4) (Figs. 3–6).

3.2. The application of the WTMM method on the stroke dataset with LE measuring

In this study, to capture the pointwise LE, the maxima are fo-cused on to identify the strongest singularity. Figs. 7–10 show the WTMM calculation with the continuous wavelet transform using the second derivative of a Gaussian wavelet. The wavelet that ful-fills this criterion is the Mexican hat wavelet. Subsequently, the WTMM determines the modulus maxima for each of the scale. The WTMM is aimed to be employed with large stroke dataset (2242×23). The normal fluctuation is frequently characterized by the positive LE; whereas the presence of strong local singularities is characterized by the negative LE [31,44].

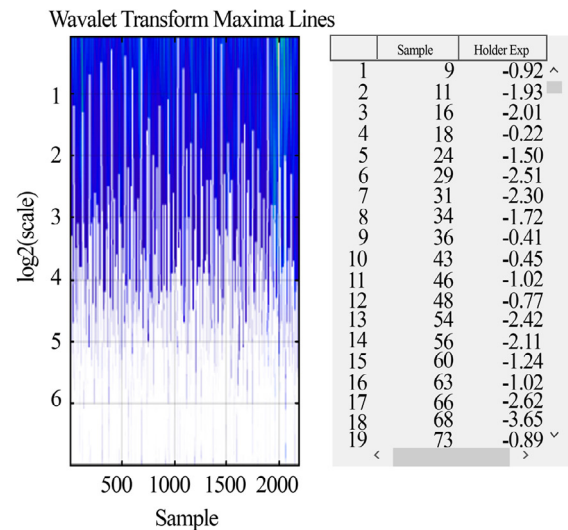
The modulus maximum at point definition x_0 [31,46,47,54,59]

$$|Wf(u, s_0)| < |Wf(u_0, s_0)|$$

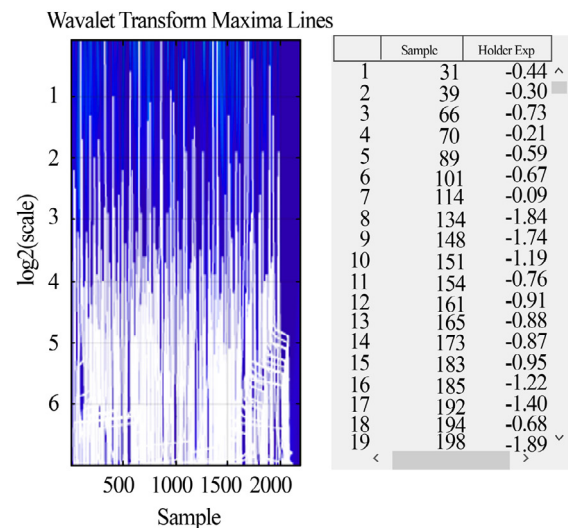
In which x is either in the left or right part of the neighborhood of x_0 . When x is in the opposite neighborhood of x_0 , the definition will be as in [46,54,59].

$$|Wf(u, s_0)| \leq |Wf(u_0, s_0)|$$

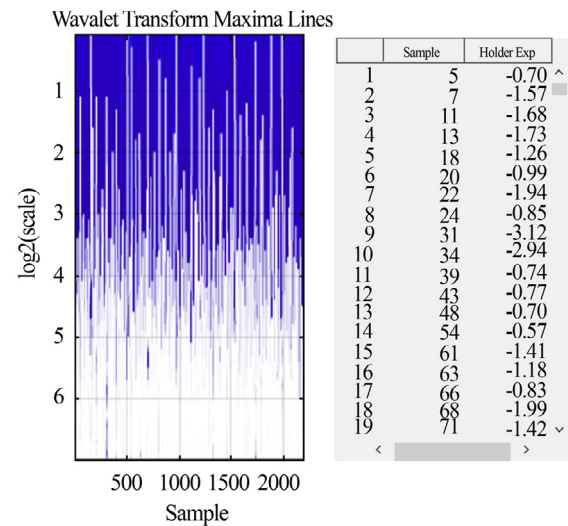
The WTMM to find the additional maxima reiterates for values in the scale. The WTMM, then, continues up through the scales which are finer, by checking if the maxima align between the scales or not. If a maximum comes closer to the finest scale, it is a true maximum and shows a singularity at that point. Besides singularity, singularity spectrum is a function which is employed



(a) Age

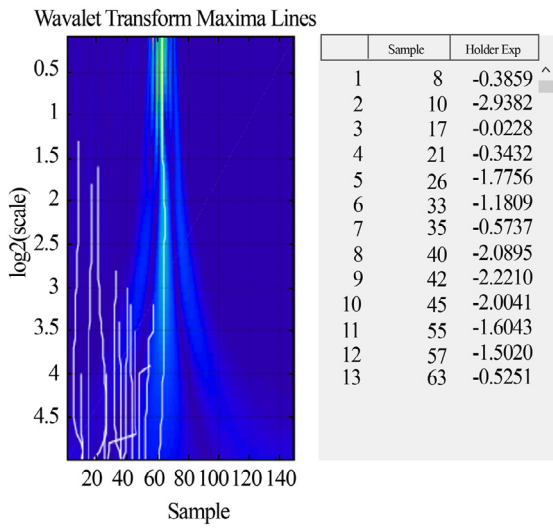


(c) Hemorrhagic Conversion

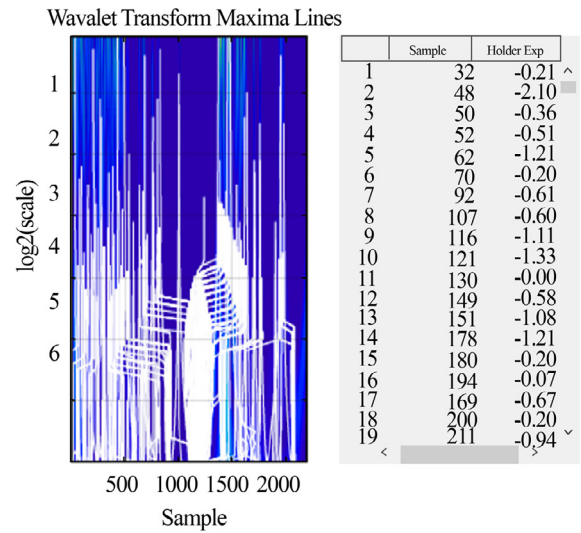


(c) Hyperlip

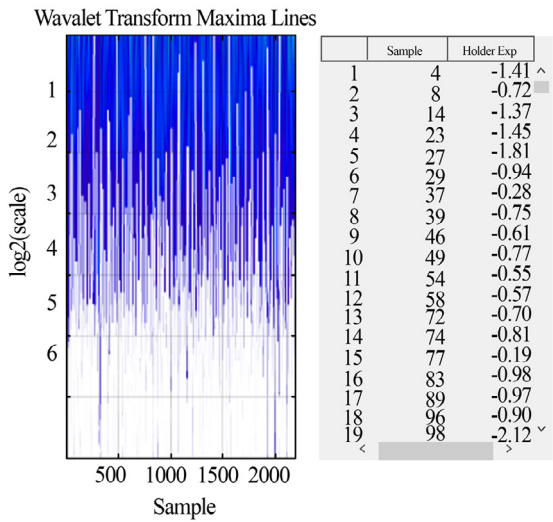
Fig. 7. log-log characteristics Modulus Maxima for attributes of WTMM_stroke dataset.



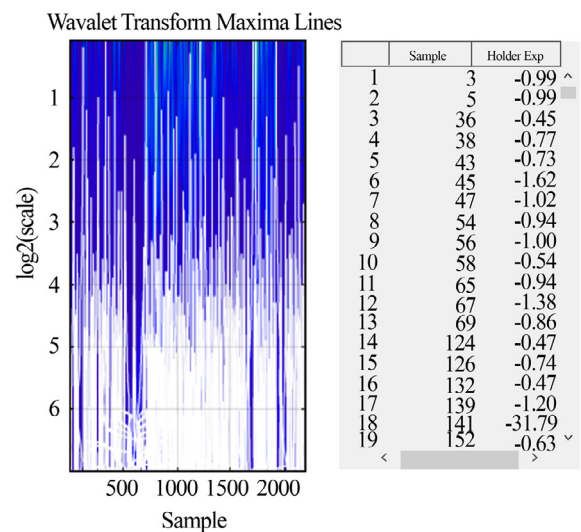
(b) ETOH



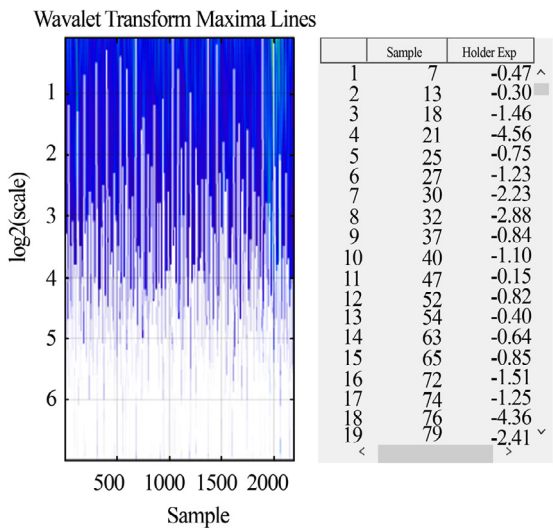
(g) mrs 90 days



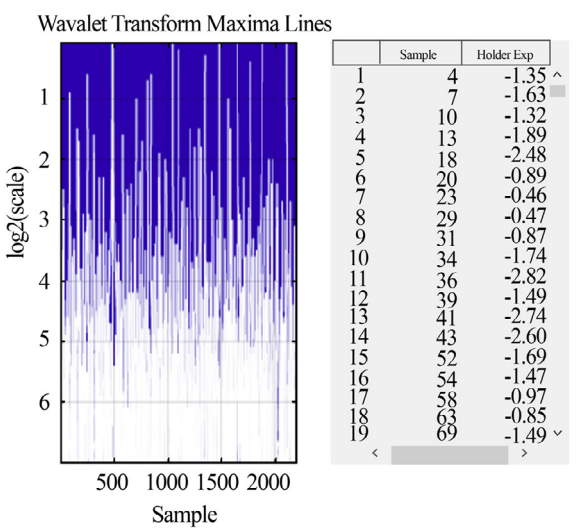
(d) H O/Stroke/TIA



(i) PAD Ca rortid



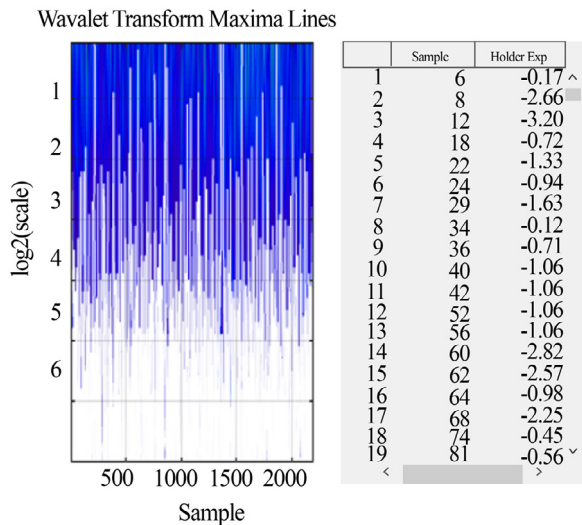
(f) IV Tpa



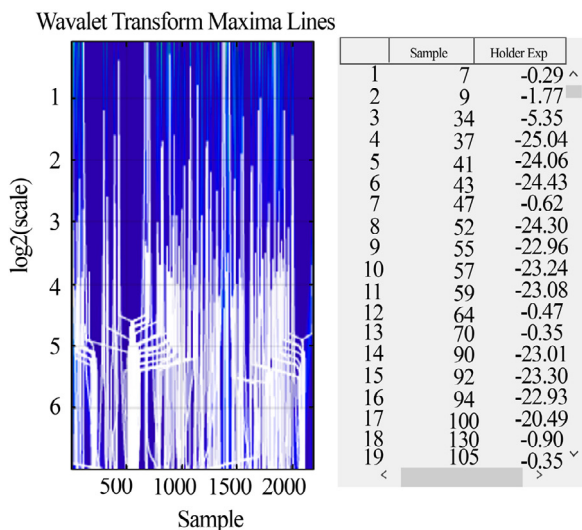
(k) Statin

Fig. 8. (Fig. 7 Cont.) log-log characteristics Modulus Maxima for attributes of WTMM_stroke dataset.

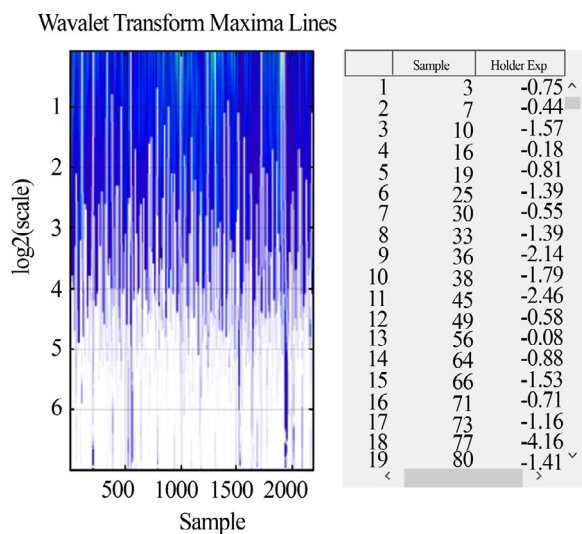
Fig. 9. (Fig. 7 Cont.) log-log characteristics Modulus Maxima for attributes of WTMM_stroke dataset.



(h)NIHSS Admission



(j) Perfusion



(l) Tobacco

Fig. 10. (Fig. 7 Cont.) log-log characteristics Modulus Maxima for attributes of WTMM_stroke dataset.

Table 5
FFBP algorithm training network properties.

ANN Network Properties	ANN Algorithms Network
	Properties Value
	stroke dataset (2242 × 23)
Input Data	BC_stroke dataset (2242 × 12)
	WTMM_stroke dataset (2242 × 12)
Training Function	Levenberg Marquardt
Adaption Learning Function	Learning Gradient Descent
Transfer Function	Tansig
Performance Function	Mean Squared Error
Hidden Layer Numbers	10
Transfer Function	Sigmoid
Epoch	1000 iteration

in multifractal analysis for the purpose of describing the fractal dimension in a subset of a function's point that pertains to a point group with the same Hölder exponent. The singularity spectrum provides a value regarding how fractal a set of points are in a function.

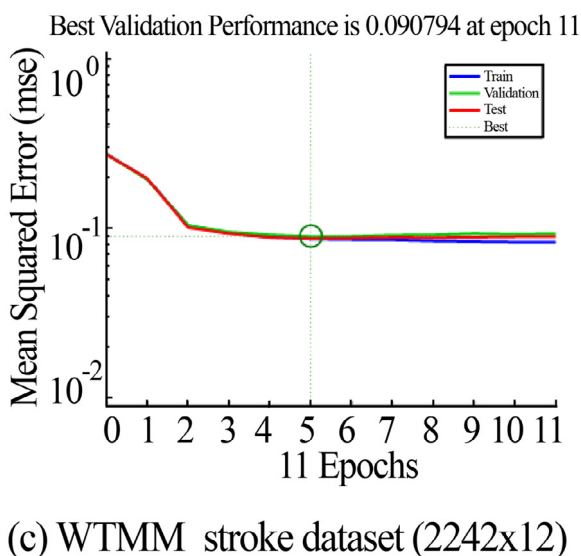
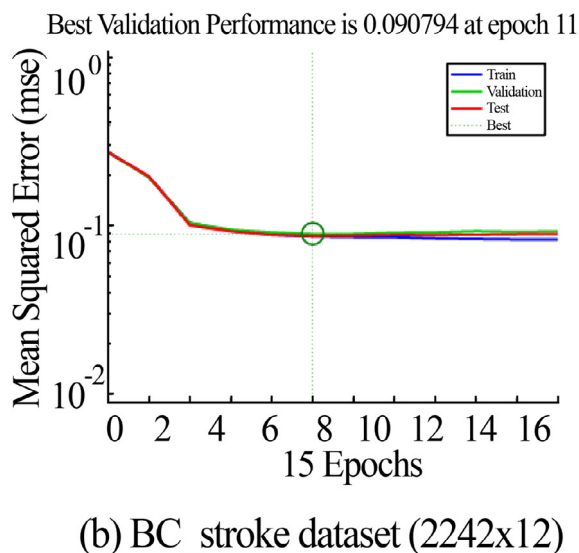
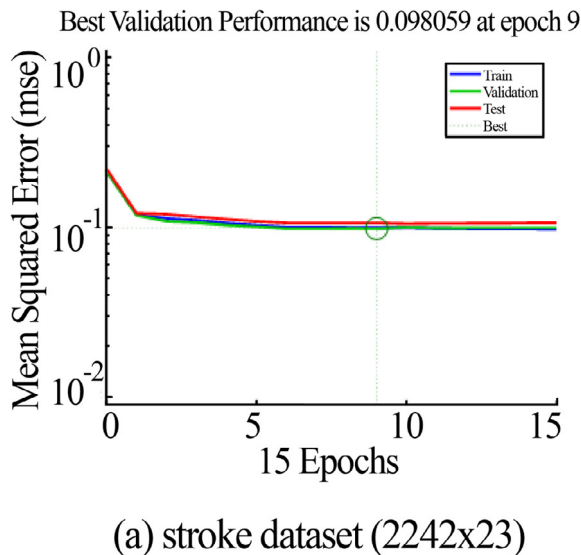
Figs. 7–10 present the WTMM_stroke dataset, obtained by the LE and plot the modulus maxima. The stroke dataset is made up of 2242 patients and 23 attributes (see Table 1). WTMM analysis has evaluated each of the 2242 patients along with 23 attributes to identify the significant attributes among them. As a result of this analysis, it has been found out that as the Hölder value increased, more differentiability was observed at the signal at that point. As the sample increased, the Hölder value decreased. When a maximum approaches the finest scale, it becomes a true maximum, presenting a singularity at that point. For the estimation of the differentiability degree of a signal's all singularities regarding the sample based on the stroke dataset. The LE at samples 1 and 2242 are very close to the values specified in the strongest regularity data (see Figs. 7–10 which depict the most significant attributes obtained). Among 23 attributes, 12 attributes (with the closest Hölder exponent values due to being significant) were selected and 11 were removed. The attributes' sample and Hölder exponent results in terms of the differentiable maxima lines directly correspond to figures and positions of singular points.

As a result of the WTMM application on the stroke dataset, the significant, efficient and regular attributes were identified. WTMM_stroke dataset (2242 × 12) was obtained from this application. The presence of strong local singularities is characterized by the negative LE. The attributes identified are: Age, ETOH, Hemorrhagic Conversion, HO/Stroke/TIA, Hyperlip, IV Tpa, mrs 90 days, NIHSS Admission, PAD Carortid, Perfusion, Statin, Tobacco (see Figs. 7–10). For transient signals, the singularities usually carry the most significant information in the transient signal's analysis [54]. As can be observed from the results obtained, the applicability and reliability of Mallat's WTMM is verified due to the fact that the singularities could be calculated from the evolution of the Wavelet transform maxima across scales.

3.3. The application of the FFBP algorithm on stroke datasets

Table 5 presents the FFBP algorithm Training Network Properties used to attain high classification accuracy rates for stroke dataset (2242 × 23), BC_stroke dataset (2242 × 12) and WTMM_stroke dataset (2242 × 12). The common parameters that yield the overall accuracy results (sensitivity, specificity, accuracy rate) in the application can be seen in detail from Table 5.

The performance graph that has been obtained from the classification of stroke dataset (2242 × 23), BC_stroke dataset (2242 × 12) and WTMM_stroke dataset (2242 × 12) by the FFBP algorithm can be seen in Fig. 11.

**Table 6**

Overall accuracy results of FFBP application on the stroke dataset, BC_stroke dataset and WTMM_stroke dataset.

Stroke datasets	Sensitivity (%)	Specificity (%)	Accuracy Rate (%)
stroke dataset (2242 × 23)	90.32 ± 4.10	90.89 ± 2.13	90.72 ± 2.13
BC_stroke dataset (2242 × 12)	90.11 ± 3.40	90.18 ± 3.02	90.93 ± 3.23
WTMM_stroke dataset (2242 × 12)	91.07 ± 4.01	91.16 ± 0.12	91.025 ± 1.25

The results of the Mean Square Error (MSE) obtained from the modelling of three stroke datasets (stroke dataset, BC_stroke dataset and WTMM_stroke dataset) by the FFBP algorithm are provided in Fig. 11. The best validation performance obtained from the stroke dataset is 0.098059 (see Fig. 11(a)). The best validation performance obtained from the application of the FFBP on the BC_stroke dataset is 0.090794 (see Fig. 11(b)). And the best validation performance obtained from the application of the FFBP on the WTMM_stroke dataset is 0.089745 (see Fig. 11(c)).

Overall, the best validation performance was observed on the WTMM_stroke dataset compared to the stroke dataset and BC_stroke dataset. The comparative results are presented in Fig. 11.

The results for Training ROC analysis, Validation ROC analysis, Test ROC analysis and All ROC analysis are presented in Fig. 12, Fig. 13 and Fig. 14 for three datasets (stroke dataset, BC_stroke dataset and WTMM_stroke dataset). The results have been obtained by the application of the FFBP algorithm regarding the classification of stroke subtypes.

3.4. The classification results of the stroke datasets with the FFBP algorithm

The overall accuracy results (sensitivity, specificity, accuracy rate) regarding the application of the FFBP algorithm on the stroke dataset, BC_stroke dataset and WTMM_stroke dataset for the classification of stroke subtypes are provided in Table 6.

The comparison results in Table 6 (Fig. 12, Fig. 13 and Fig. 14) show that the stroke dataset achieved a sensitivity of $90.32 \pm 4.10\%$, specificity of $90.89 \pm 2.13\%$, and accuracy of $90.72 \pm 2.13\%$. The BC_stroke dataset achieved sensitivity of $90.11 \pm 3.40\%$, specificity of $90.18 \pm 3.02\%$, and accuracy of $90.93 \pm 3.23\%$. The WTMM_stroke dataset achieved a sensitivity of $91.07 \pm 4.01\%$, a specificity of $91.16 \pm 0.12\%$, and an accuracy of $91.025 \pm 1.25\%$. Therefore, it is obvious that using WTMM_stroke dataset obtained larger sensitivity, specificity, and accuracy than the stroke dataset, BC_stroke dataset. It may also be concluded that WTMM is superior to BC in terms of classification accuracy rate for stroke subtypes.

Overall, the aim of this study is to classify the 8 stroke subtypes based on the identification of efficient, regular, self-similar and significant attributes. Considering the life-threatening risk and aspect of stroke as a medical problem, accurate classification is of vital importance for the survival and life quality of the patient. Accurate classification means accurate and early diagnosis, thus, a higher level of accuracy in classification. For this aim, identifying the most significant, efficient, self-similar and regular attributes in the stroke dataset (see Tables 1 and 2) will make a significant difference for both the patients and the clinicians. The results show that WTMM_stroke dataset which comprised of significant, efficient, self-similar and regular attributes yielded the highest results for classification in terms of accuracy compared to the two other datasets, which are stroke dataset and BC_stroke dataset.

Fig. 11. FFBP algorithm performance graph (a) stroke dataset (b) BC_stroke dataset (c) WTMM_stroke dataset.

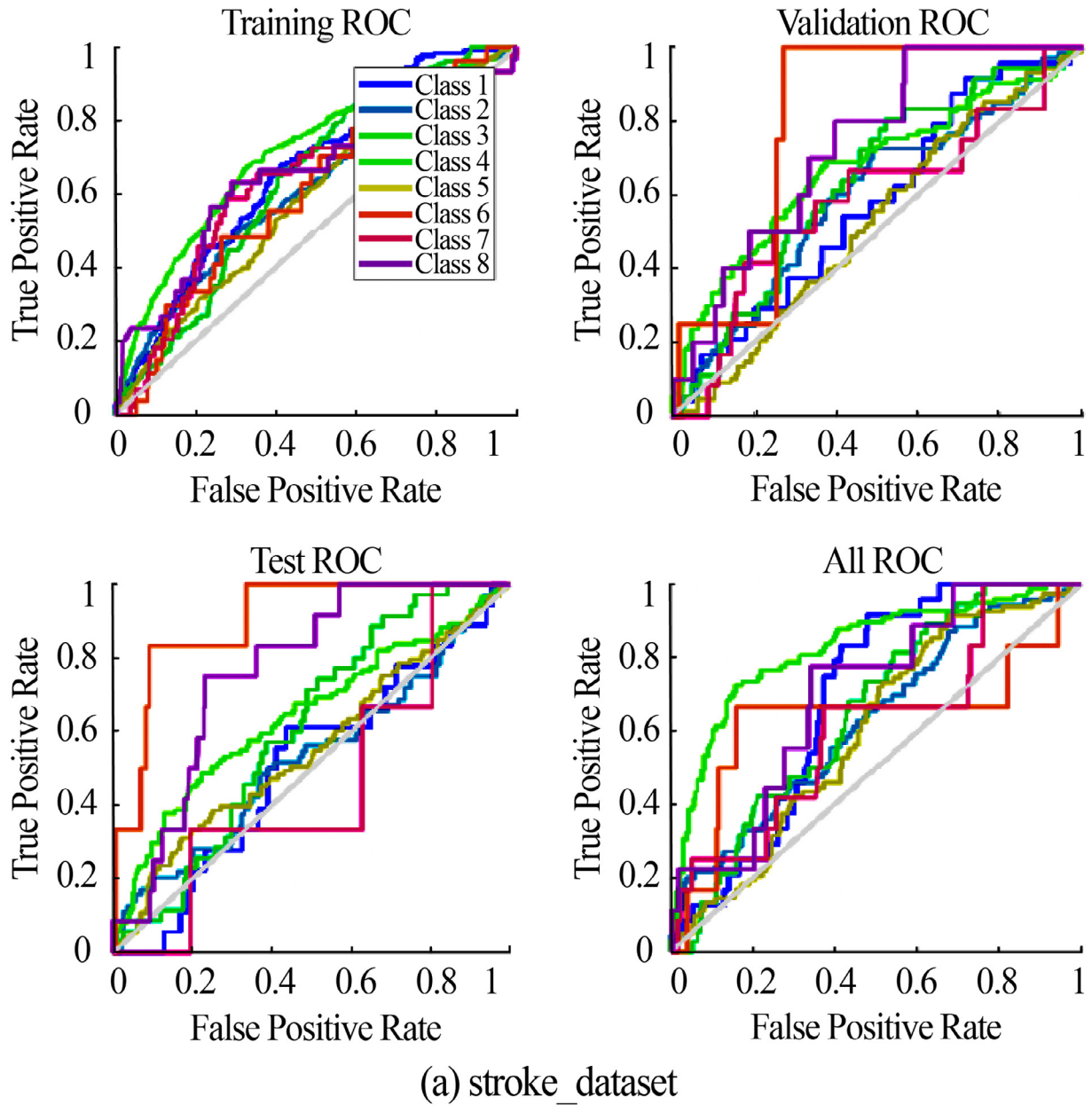


Fig. 12. Results of the Training ROC, Validation ROC analysis Test ROC analysis and All ROC analysis for (a) stroke dataset (b) BC_stroke dataset (c) WTMM_stroke dataset.

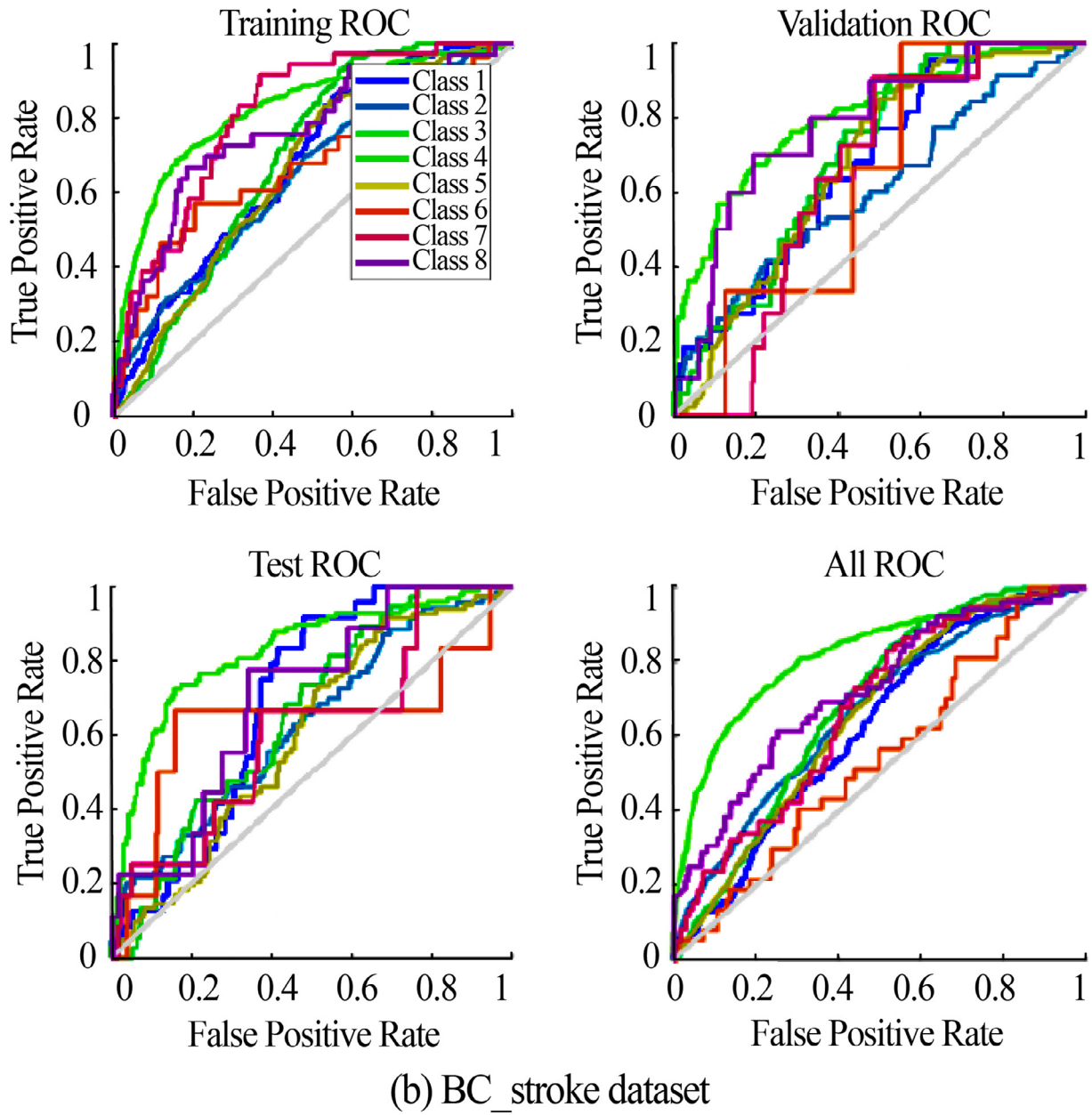


Fig. 13. (Fig. 12 Cont.) Results of the Training ROC, Validation ROC analysis Test ROC analysis and All ROC analysis for (a) stroke dataset (b) BC_stroke dataset (c) WTMM_stroke dataset.

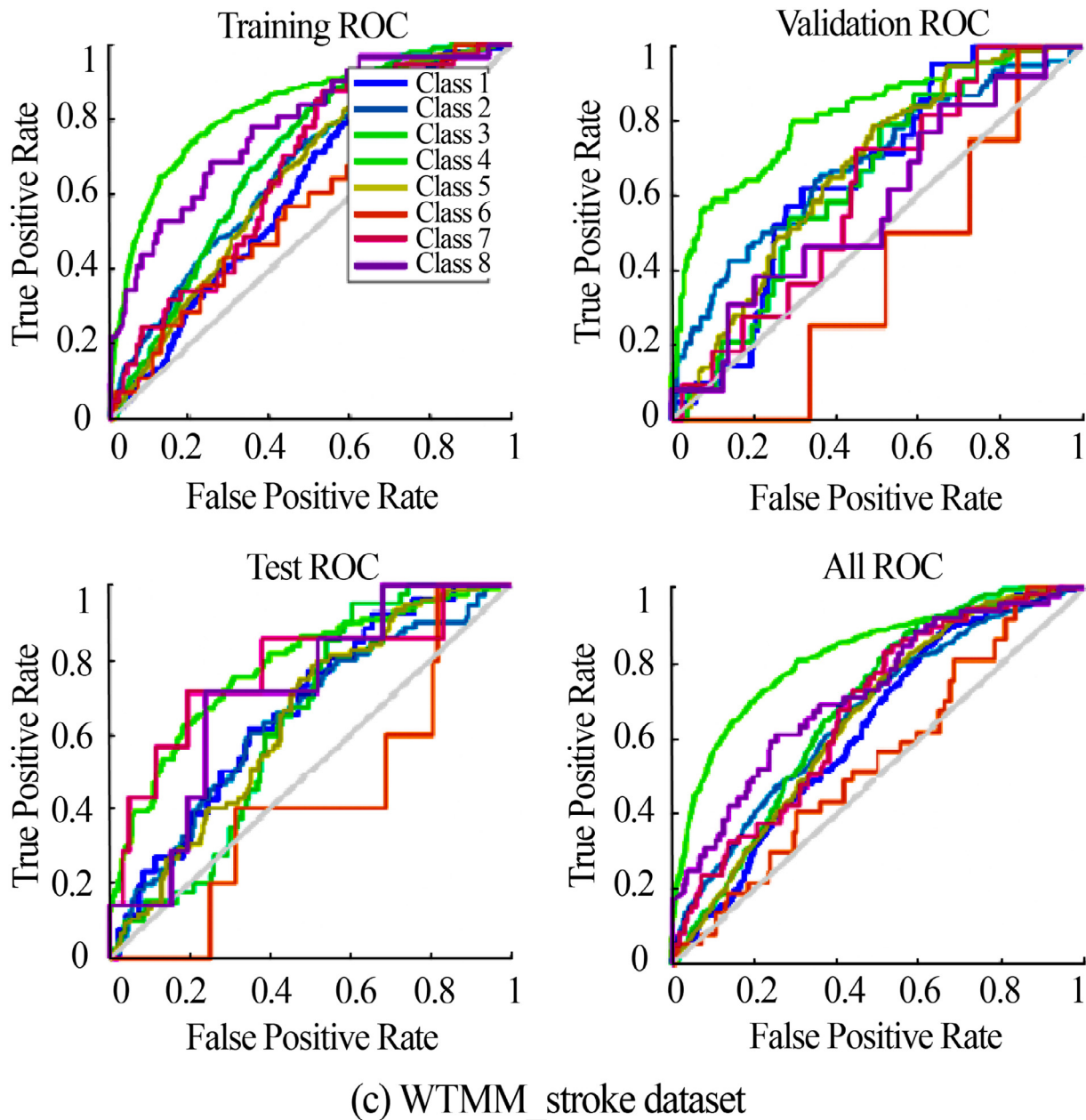


Fig. 14. (Fig. 12 Cont.) Results of the Training ROC, Validation ROC analysis, Test ROC analysis and All ROC analysis for (a) stroke dataset (b) BC_stroke dataset (c) WTMM_stroke dataset.

4. Conclusion

The principal contribution the study has been to employ an applicable approach with multifarious and integrated methodology for the purpose of stroke subtypes' classification. The originality of this study is due to the fact that no study exists in the literature in which BC and WTMM methods have been employed. Regarding the contributions in terms of approaches in this study, initially, the Box-counting dimension and Wavelet transform modulus maxima, which are among the fractal and multifractal methods, were applied in order to calculate the self-similar and regular data from the stroke dataset (224×23). Thereby, regular, self-similar, efficient and significant attributes in stroke dataset were identified by the two initial methods, namely BC and WTMM. Two datasets, BC_stroke dataset (2242×12) and WTMM_stroke

dataset (2242×12), were obtained accordingly. It is, therefore, the first time these methods have been employed on such an extensive stroke data for the detection of the singularities in the stroke datasets. The singularity spectrum provides a value concerning how fractal a set of points are in the BC_stroke dataset (2242×12) and WTMM_stroke dataset (2242×12). When compared with the other relevant works [11,39,41–44] done up until now, the present study has provided these novel aspects. The second contribution in terms of the methods in the approach includes classification performed using one of the ANN algorithms, namely FFBP. The aim of using this algorithm in this second methodological approach is to apply accurate classification of the stroke subtypes. The applications ensure the attainment of the most regular, self-similar, efficient and significant attributes for the stroke subtype classification. ANN was applied on stroke dataset, BC_stroke

dataset (2242×12) and WTMM_stroke dataset (2242×12), thus, classification has been done for the subtypes of stroke through accuracy rates (based on sensitivity and specificity). The results of the study demonstrated that the classification accuracy rate obtained for WTMM_stroke dataset (2242×12), has proven to be higher than that of stroke dataset (2242×23) and BC_stroke dataset (2242×12). These results underline the importance of selecting significant attributes for the classification of a critical and potentially fatal disease which might end up with deaths. The aforementioned methods have been used for the first time for this particular stroke dataset in this study. Besides this, it is seen that no work has been reported yet which examines such a comprehensive stroke dataset that relates attributes (demographic information, medical history, results of laboratory tests, treatments, and medications). The study also provides a novelty in this regard. Experimental results reveal the validity, accuracy and applicability of the proposed method.

Each data has a distinctive nature, in particular for data such as stroke, which includes brain as a complex structure requiring complexity analysis, the selection of right method to analyse the data properly plays a critical role. Due to transient attributes of stroke as well as other neurological handled in medical analyses, fractal and multifractional approaches enable the development and application of alternative adaptive models, which define modern neuroscience.

Based on these considerations, the following directions may be provided for future research:

- (1) The combination of methods and proposed model demonstrates that WTMM is apparently a critical determining method compared to BC method for enhancing classification with respect to the identification of self-similar and regular attributes. With this perspective, it could be possible for future research to focus on different data sets in several other areas.
- (2) Apart from the WTMM and Box-Counting used in this study for the singularity spectrum detection, additional reliable fractal and multifractional methods such as Modified Multifractal Detrended Fluctuation Analysis (MFDFA), Diffusion Limited Aggregation (DLA) and so forth can be employed for future work to obtain comparative results.
- (3) The proposed model can illustrate a direction for researchers to pay attention to the selection of most significant attributes for diagnostic purposes.
- (4) The model presented in this study may be addressed as interface(s) in the models to be used like the study in [41] in the future.
- (5) The results and the model constructed with the integrated methodology may provide a direction for the diagnosis of diseases, classification of them and robust prediction processes.
- (6) The proposed model can present a novel direction for future works and projects that will integrate advanced mathematical models and artificial intelligence techniques.

Taking all these into consideration, the study aims at pointing a new direction in the relevant fields concerning the complex dynamic systems and structures. Considering the importance of accuracy in classification and timely diagnosis for the life quality of the stroke patients, the present study has attempted to abridge a gap in the literature and provide a new frontier in modern neuroscience.

5. Limitation

The stroke dataset in our study is big data (2242 patients and 23 attributes) (see Table 1). The results obtained from the WTMM analyses shown in detail in Figs. 7–10 depict only the attributes

identified as significant WTMM_stroke dataset (2242×12). Due to the space restriction for the figures to fit in, it has not been able to depict all of the attributes' sample and Hölder exponent results in terms of the differentiable maxima lines.

Declaration of Competing Interest

The authors declare that they have no known competing financial interests or personal relationships that could have appeared to influence the work reported in this paper.

References

- [1] Ieva AD, Esteban FJ, Grizzi F, Klonowski W, Martin-Landrove M. Fractals in the neurosciences, part II: clinical applications and future perspectives. *Neuroscientist* 2015;21(1):30–43. doi:10.1177/1073858413513928.
- [2] Ai T, Zhang R, Zhou HW, Pei JL. Box-counting methods to directly estimate the fractal dimension of a rock surface. *Appl Surf Sci* 2014;314:610–21. doi:10.1016/j.apsusc.2014.06.152.
- [3] Ristanovic D, Stefanovic BD, Puskas N. Fractal analysis of dendrite morphology using modified box-counting method. *Neurosci Res* 2014;84:64–7. doi:10.1016/j.neures.2014.04.005.
- [4] Karaca Y, Cattani C, Moonis M, Bayrak S. Stroke subtype clustering by multifractal bayesian denoising with fuzzy c means and k-means algorithms. *Complexity* 2018. doi:10.1155/2018/9034647.
- [5] Zhang YD, Zhang Y, Phillips P, Dong Z, Wang S. Synthetic minority oversampling technique and fractal dimension for identifying multiple sclerosis. *Fractals* 2017;25(04):1740010. doi:10.1142/S0218348X17400102.
- [6] Karaca Y, Cattani C. *Computational methods for data analysis*. Walter de Gruyter GmbH, Berlin/Boston + co-pub; 2018. p. 978–3110496352.
- [7] Karaca Y, Cattani C. Clustering multiple sclerosis subgroups with multifractal methods and self-organizing map algorithm. *Fractals* 2017;25(4):1740001. doi:10.1142/S0218348X17400011.
- [8] Yin J, Li Y, Cui H. Box-counting dimensions and upper semicontinuity of bi-spatial attractors for stochastic degenerate parabolic equations on an unbounded domain. *J Math Anal Appl* 2017;450(2):1180–207. doi:10.1016/j.jmaa.2017.01.064.
- [9] Sudha A, Gayathri P, Jaisankar N. Effective analysis and predictive model of stroke disease using classification methods. *Int J Comput Appl* 2012;43(14):26–31. doi:10.5120/6172-8599.
- [10] Moonis M, Husaini B. The impact of co-morbid sleep apnea and stroke on the cost of health care. 2018. P1. 091.
- [11] Almadani O, Alshammari R. Prediction of stroke using data mining classification techniques. *Int J Adv Comput Sci Appl* 2018;9(1):457–60. doi:10.14569/IJACSA.2018.090163.
- [12] Silver B, Hamid T, Napoli M.D., Behrouz R, Khan M., Saposnik G., Moonis M. Twelve versus twenty four hour bed rest after acute ischemic stroke reperfusion therapy. 2018. P5, 204.
- [13] Barbui T, De Stefano V, Carobbio A, Lazzaro VD, Guglielmelli P, Loscocco GG, et al. Short and long-term risk of major cardiovascular events after ischemic stroke or transient ischemic attack in myeloproliferative neoplasms. *Am Soc Hematol* 2017;130(202). doi:10.1038/s41408-018-0048-9.
- [14] Uchino K, Hernandez AV. Dabigatran association with higher risk of acute coronary events: meta-analysis of noninferiority randomized controlled trials. *Arch Intern Med* 2017;172(5):397–402. doi:10.1001/archinternmed.2011.1666.
- [15] Novaes MM, Palhano-Fontes F, Peres A, Mazzetto-Betti K, Pelicioni M, Andrade KC, et al. Neurofunctional changes after a single mirror therapy intervention in chronic ischemic stroke. *Int J Neurosci* 2018;1–9. doi:10.1080/00207454.2018.1447571.
- [16] Henninger N, Lin E, Haussen DC, Lehman LL, Takhtani D, Selim M, Moonis M. Leukoaraiosis and sex predict the hyperacute ischemic core volume. *Stroke* 2013;44(1):61–7. doi:10.1161/STROKEAHA.112.679084.
- [17] Yamanaka H, Kawahira K, Arima M, Shimodozono M, Etoh S, Tanaka N, Tsujio S. Evaluation of skilled arm movements in patients with stroke using a computerized motor-skill analyser for the arm. *International Journal of Rehabilitation Research* 2005;28(3):277–83. PMID: 16046924
- [18] Ay H. Advances in the diagnosis of etiologic subtypes of ischemic stroke. *Current neurology and neuroscience reports* 2010;10(1):14–20. PMID: PMC2861780
- [19] Millicic S. Box-counting dimensions of generalised fractal nests. *Chaos Solitons Fractals* 2018;113:125–34. doi:10.1016/j.chaos.2018.05.025.
- [20] Rajkovic N, Krstonosic B, Milosevic N. Box-counting method of 2d neuronal image: method modification and quantitative analysis demonstrated on images from the monkey and human brain. *Comput Math Methods Med* 2017. doi:10.1155/2017/8967902.
- [21] Lopes R, Betrouni N. Fractal and multifractal analysis: a review. *Med Image Anal* 2009;13(4):634–49. doi:10.1016/j.media.2009.05.003.
- [22] Karthik CKR. Characterization of stroke lesion using fractal analysis. *Asian J Pharm Clin Res* 2017;10(13):53–6. doi:10.22159/ajpcr.2017.v10s1.19558.
- [23] Zhou R, Luo Y, Fenster A, Spence JD, Ding M. Fractal dimension based carotid plaque characterization from three-dimensional ultrasound images. *Med Biol Eng Comput* 2019;57(1):135–46. doi:10.1007/s11517-018-1865-5.

- [24] Das N, Chatterjee S, Kumar S, Pradhan A, Panigrahi P, Vitkin IA, et al. Tissue multifractality and born approximation in analysis of light scattering: a novel approach for precancers detection. *Sci Rep* 2014;4(1):1–7. doi:10.1038/srep06129.
- [25] Mukhopadhyay S, Das N, Kurmi I, Ghosh N, Pradhan A, Panigrahi PK. Tissue multifractality and hidden markov model based integrated framework for optimum precancer detection. *J Biomed Opt* 2017;22(10):105005. doi:10.1117/1.JBO.22.10.105005.
- [26] Foroutan-pour K, Dutilleul P, Smith DL. Advances in the implementation of the box-counting method of fractal dimension estimation. *Appl Math Comput* 1999;105(2–3):195–210. doi:10.1016/S0096-3003(98)10096-6.
- [27] Pirici D, Mogoanta L, Margaritescu O, Pirici I, Tudorica V, Coconu M. Fractal analysis of astrocytes in stroke and dementia. *Romanian Journal of Morphology and Embryology* 2009;50(3):381–90. PMID: 19690763
- [28] Venkatakrishnan PSSMS, Sangeetha S, Sundar M. Measurement of lipschitz exponent (LE) using wavelet transform modulus maxima (WTMM). *International Journal of Scientific and Engineering Research* 2012;3(6). ISSN 2229-5518
- [29] Chirag J. Multifractal analysis of heart rate variability using wavelet-transform modulus-maxima method. M. S. Thesis. Newark, New Jersey: Biomedical Engineering Depart., New Jersey Institute of Technology; 2005.
- [30] Xingwei Y, Dawei L, Jianping O, Jun Z, Jianwei W. Singularity detection of noisy signals based on two wavelet denoising algorithms. In: *IET International Conference on Information and Communications Technologies (IETICT 2013)*. China: Beijing; 2013. p. 88–93. Doi: 10.1049/cp.2013.0039
- [31] Muzy JF, Bacry E, Arneodo. Multifractal formalism for fractal signals - the structure function approach versus the wavelet-transform modulus-maxima method. *Phys Rev E* 1993;47(2):875–84. doi:10.1103/PhysRevE.47.875.
- [32] Arneodo A, Bacry E, Muzy JF. The multifractal formalism revisited with wavelets. *Int J Bifurcation Chaos* 1994;4(2):245–302. doi:10.1142/S0218127494000204.
- [33] Ivanov PC, Rosenblum MG, Amaral LAN, Struzik ZR, Havlin S, Goldberger AL, Stanley HE. Multifractality in human heartbeat dynamics. *Nature* 1999;399:461–5. doi:10.1038/20924.
- [34] Venkatakrishnan P, Sangeetha S, Gnanasekaran JS, Vishnukumar MG, Padmanaban AS. Analysis of vibration in gearbox sensor data using lipschitz exponent (LE) function: a wavelet approach. *IFAC Proc Vol* 2014;47(1):1067–71. doi:10.3182/20140313-3-IN-3024.00102.
- [35] Pavlov AN, Abdurashitov AS, Sindeeva OA, Sindeev SS, Pavlova ON, Shihalov GM, et al. Characterizing cerebrovascular dynamics with the wavelet-based multifractal formalism. *Physica A* 2016;442:149–55. doi:10.1016/j.physa.2015.09.007.
- [36] Jian-xun Li, Xi-zheng KE. An accumulative method of pulsar standard profile based on wavelet-modulus-maxima correlation information. *Chin Astron Astrophy* 2009;33(2):158–67. doi:10.1016/j.chinastron.2009.03.008.
- [37] Sarkar T, Khondekar MH, Banerjee S. Wavelet based fractal analysis of solar wind speed signal. In: *in recent trends in signal and image processing*. Singapore: Springer; 2019. p. 39–48. Doi: 10.1007/978-981-10-8863-6_5
- [38] Sahoo S, Kanungo B, Behera S, Sabut S. Multiresolution wavelet transform based feature extraction and ECG classification to detect cardiac abnormalities. *Measurement* 2017;108:55–66. doi:10.1016/j.measurement.2017.05.022.
- [39] Shanthi D, Sahoo G, Saravanan N. Designing an artificial neural network model for the prediction of thrombo-embolic stroke. *Int J BiometrBioinform (IJBB)* 2009;3(1):10–18. doi:10.5220/0003875304670470.
- [40] Colak C, Karaman E, Turtay MG. Application of knowledge discovery process on the prediction of stroke. *Comput Methods Programs Biomed* 2015;119(3):181–5. doi:10.1016/j.cmpb.2015.03.002.
- [41] Karaca Y, Moonis M, Zhang YD, Gezgez C. Mobile cloud computing based stroke healthcare system. *Int J Inf Manage* 2019;45:250–61. doi:10.1016/j.ijinfomgt.2018.09.012.
- [42] Mirtskhulava L, Wong J, Al-Majeed S, Pearce G. Artificial neural network model in stroke diagnosis. In: *In 2015 17th UKSim-AMSS International Conference on Modelling and Simulation*; 2015. p. 50–3. Doi: 10.1109/UKSim.2015.33
- [43] Bong SZ, Wan K, Murugappan M, Ibrahim NM, Rajamanickam Y, Mohamad K. Implementation of wavelet packet transform and non linear analysis for emotion classification in stroke patient using brain datas. *Biomed Data Process Control* 2017;36:102–12. doi:10.1016/j.bspsc.2017.03.016.
- [44] Pavlov AN, Abdurashitov AS, Sindeeva OA, Sindeev SS, Pavlova ON, Shihalov GM, et al. Characterizing cerebrovascular dynamics with the wavelet-based multifractal formalism. *Physica A* 2016;442:149–55. doi:10.1016/j.physa.2015.09.007.
- [45] The mathworks, MATLAB (r2018b). 2018. The mathWorks, inc., natick, MA
- [46] Vehel J.L. 2018. FraLab, [Online]. Available: project.inria.fr/fraclab/.
- [47] Foroutan-pour K, Dutilleul P, Smith DL. Advances in the implementation of the box-counting method of fractal dimension estimation. *Appl Math Comput* 1999;105(2–3):195–210. doi:10.1016/S0096-3003(98)10096-6.
- [48] Stephen W. Diagnosing ASD with fractal analysis. *Adv Autism* 2017;3(1):47–56. doi:10.1108/AIA-03-2016-0007.
- [49] Mallat S. *A wavelet tour of data processing*. Academic press; 1999.
- [50] Karaca Y. Wavelet-based multifractal spectrum estimation in hepatitis virus classification models by using artificial neural network approach. *Global Virology III: Virology in the 21st Century*. Shapshak P, Balaji S, Somboonwit C, Chiappelli F, Menezes L, Kanguane P, Sinnott J, editors. Springer; 2019. Doi.org/10.1007/978-3-030-29022-1_4
- [51] Peng ZK, Chu FL, Peter WT. Singularity analysis of the vibration signals by means of wavelet modulus maximal method. *Mech Syst Signal Process* 2007;21(2):780–94. doi:10.1016/j.ymsp.2005.12.005.
- [52] So GB, So HR, Jin GG. Enhancement of the box-counting algorithm for fractal dimension estimation. *Pattern Recognit Lett* 2017;98:53–8. doi:10.1016/j.patrec.2017.08.022.
- [53] Xu J, Jian Z, Lian X. An application of box counting method for measuring phase fraction. *Measurement* 2017;100:297–300. doi:10.1016/j.measurement.2017.01.008.
- [54] Mandelbrot BB. Self-affine fractals and fractal dimension. *Phys Scr* 2006;32(4):257. doi:10.1088/0031-8949/32/4/001.
- [55] Sanderson BG, Booth DA. The fractal dimension of drifter trajectories and estimates of horizontal eddy-diffusivity. *Tellus A* 1991;43(5):334–49. doi:10.1034/j.1600-0870.1991.t01-1-00008.
- [56] Liebowitch LS, Toth T. A fast algorithm to determine fractal dimensions by box counting. *Phys Lett A* 1989;141(8–9):386–90. doi:10.1016/0375-9601(89)90854-2.
- [57] Jaffard S, Lashermes B, Abry P. Wavelet leaders in multifractal analysis. In: Qian T, Vai MI, Xu Y, editors. *Applied and Numerical Harmonic Analysis*. Birkhauser Basel; 2006. p. 201–46. Doi:10.1007/978-3-7643-7778-6_17
- [58] Mallat S, Hwang WL. Singularity detection and processing with wavelets. *IEEE Trans Inf Theory* 1992;38(2):617–43. doi:10.1109/18.119727.
- [59] Bujanovic T, Abdel-Qader I. On wavelet transform general modulus maxima metric for singularity classification in mammograms. *Open J Med Imaging* 2013;3(1):17. doi:10.4236/ojmi.2013.31004.
- [60] Pavlova ON, Abdurashitov AS, Ulanova MV, Shushunova NA, Pavlov AN. Effects of missing data on characterization of complex dynamics from time series. *Commun Nonlinear Sci Numer Simul* 2019;66:31–40. doi:10.1016/j.cnsns.2018.06.002.
- [61] Jaffard S. Pointwise smoothness, two-microlocalization and wavelet coefficients. *Publicacions Matemàtiques* 1991;35(1):155–68. doi:10.5565/PUBLMAT_35191_06.
- [62] Jaffard S. Exponent de h lder et coefficients d' ondelettes. In: (h lder exponents and wavelet coefficients"), vol. 308. C. R. Academie des Sciences; 1989. p. 79–81.
- [63] . Wavelets, fractals and fourier transforms. Farge M, Hunt JCR, Vassilicos JC, editors. 1st ed. Oxford University Press; 1993. ISBN-13: 978-0198536475
- [64] Yuan YT, Li BF, Ma H, Lin J. Ring-projection-wavelet-fractal signatures: a novel approach to feature extraction. *IEEE TransCircuits Syst II* 1998;45(8):1130–4. doi:10.1109/82.718824.
- [65] Jaffard S, Melot C. Wavelet analysis of fractal boundaries. part 1: local exponents. *Commun Math Phys* 2005;258(3):513–39. doi:10.1007/s00220-005-1354-1.
- [66] Qijun X, Wei H, Zhonghui L, Yanghua L, Canyi D. Wavelet transform singularity detection technology applied in the seabed sediment sound velocity measurement. In: *12th IEEE Conf on In Industrial Electronics and Applications (ICIEA)*, 2017. Cambodia: Siem Reap; 2017. p. 1050–4. doi:10.1109/ICIEA.2017.8282994.
- [67] Vrscay ER. A generalized class of fractal-wavelet transforms for image representation and compression. *Can J Electr Comput Eng* 1998;23(1–2):69–83. doi:10.1109/CJECE.1998.7102047.
- [68] Ramirez-Pacheco JC, Trejo-Sanchez JA, Cortez-Gonzalez J, Palacio RR. Classification of fractal signals using two-parameter non-extensive wavelet entropy. *Entropy* 2017;19(5):224. doi:10.3390/e19050224.
- [69] Lee CM, Zhang YT. Reduction of motion artifacts from photoplethysmographic recordings using a wavelet denoising approach. In: *IEEE EMBS Asian-Pacific Conf on Biomedical Engineering*. JAPAN: Kyoto-Osaka-Nara; 2003. p. 194–5. Doi: 10.1109/APBME.2003.1302650
- [70] Hagan MT, Menhaj MB. Training feedforward networks with the marquardt algorithm. *IEEE Trans Neural Networks* 1994;5(6):989–93. doi:10.1109/72.329697.
- [71] Karaca Y, Cattani C. A comparison of two h lder regularity functions to forecast stock indices by ANN algorithms. In: Misra S, et al., editors. *19th In International Conf. on Computational Science and Its Applications*. Saint Petersburg, Russia, vol 11620. Cham: Springer; 2019. p. 270–84. Doi.org/10.1007/978-3-030-24296-1_23
- [72] Saeedi E, Hossain MS, Kong Y. Feed-forward back-propagation neural networks in side-channel information characterisation. *J Circuits Syst Comput* 2019;28(1). doi:10.1142/S0218126619500038.



Y. Karaca is an Assistant Professor of Applied Mathematics. She is currently a researcher at the University of Massachusetts Medical School (UMASS), USA. Her research interests include computational methods, mathematical neuroscience, medical analyses, fractals, wavelets, entropy, stochastic analyses as well as complex systems.



M. Moonis is a professor at the University of Massachusetts Medical School (UMASS), Department of Neurology. As a neurologist in Worcester, Massachusetts, he has been affiliated with multiple hospitals in the area, including Health Alliance Hospital and UMass Memorial Medical Center. In 1999, he became the Director at the Stroke Prevention Clinic, UMass Memorial Medical Center. He also holds positions as a reviewer and editor for the editorial boards of many acknowledged national and international SCI journals.



D. Baleanu is a professor at the Institute of Space Sciences, Magurele-Bucharest, Romania and a visiting staff member at the Department of Mathematics, Cankaya University, Ankara, Turkey. His fields of interest include the fractional dynamics and its applications in science and engineering, fractional differential equations, discrete mathematics, mathematical physics, soliton theory, Lie symmetry, dynamic systems on time scales and the wavelet method and its applications.